Review

Developments of GNSS buoy for a synthetic geohazard monitoring system

By Teruyuki KATO,[*1,†] Yukihiro TERADA,[*2] Keiichi TADOKORO[*3] and Akira FUTAMURA[*4]

(Edited by Yoshio FUKAO, M.J.A.)

Abstract: A global navigation satellite system (GNSS) buoy system for early tsunami warnings has been developed for more than 20 years. The first GNSS buoy system using a real-time kinematic algorithm (RTK) was implemented in the Nationwide Ocean Wave information network for Ports and HArbourS (NOWPHAS) wave monitoring system in Japan in 2008. The records of NOWPHAS were used to update the tsunami alert by the Japan Meteorological Agency (JMA), owing to the tsunami generated by the 2011 Tohoku-oki earthquake (Mw9.0). However, considering that the distance limit is less than 20 km for the RTK algorithm, a new system was designed by introducing a new positioning algorithm and satellite data transmission to place the buoy much farther from the coast. A new technique for the continuous monitoring of ocean-bottom crustal movements was also implemented in the new system. The new buoy system can be used for weather forecasting and ionospheric monitoring as well.

Keywords: GNSS buoy, tsunami, tsunami early warning, GNSS-Acoustic measurements, geohazard monitoring

1. Introduction

The Japanese Islands have been attacked by frequent large earthquakes and resultant tsunamis. Along the northeastern Pacific coast, the 1896 Meiji Sanriku earthquake (Mw8.4), 1933 Showa Sanriku earthquake (Mw8.4), and the 2011 off the Pacific coast of Tohoku earthquake (Mw9.0) (hereinafter called the Tohoku-oki earthquake) are eminent examples. In southwestern Japan, numerous tsunamigenic earthquakes have occurred along the coast, including the 1946 Nankai earthquake (Mw8.4) as the recent case. These earthquakes occurred along the plate interface between the subducting oceanic plate and the overriding continental plate. There are less frequent but significant tsunamigenic earthquakes along the Japan Sea coasts as well. The 1983 Nihonkai-Chubu earthquake (Mw7.7) and the 1993 Hokkaido Nansei-oki earthquake (Mw7.7) are recent examples.

Though there are few cases where volcanic eruptions or large landslides in the ocean cause tsunamis, most tsunamis are generated by crustal movements caused by large earthquakes at ocean floors. As water is incompressible, the sea water above the ocean-bottom crustal deformation is vertically displaced according to the crustal motion at the ocean floor, generating a tsunami. If the magnitude of the earthquake exceeds 8, the generated wave has meters in height amplitude and tens to hundreds of kilometers in wavelength. Moreover, the tsunami heights are amplified as they move toward the shallower coastal area, causing casualties and destroying properties. Mitigating such disasters is a crucial and socially important element in Japan and other threatened areas worldwide.

To reduce disasters due to tsunamis, various countermeasures against tsunamis should be developed. For example, a tsunami alert is issued as

[*1] Institute of Regional Development, Taisho University, Tokyo, Japan.
[*2] National Institute of Technology, Kochi College, Kochi, Japan.
[*3] Graduate School of Environmental Studies, Nagoya University, Nagoya, Aichi, Japan.
[*4] National Institute of Technology, Yuge College, Ehime, Japan.
[†] Correspondence should be addressed: T. Kato, Institute of Regional Development, Taisho University, 3-20-1 Nishi-Sugamo, Toshima-ku, Tokyo 170-8470, Japan (e-mail: t_kato@mail.tais.ac.jp).

quickly as possible after the occurrence of a large earthquake at the ocean floor. In Japan, the Japan Meteorological Agency (JMA) is responsible for issuing early tsunami warnings for such large earthquakes, and the JMA issued the first tsunami alert in 1941.[1] Currently, they attempt to issue such alerts within a few minutes after the onset of an earthquake. The decision to issue alerts is made based on the earthquake source parameters, such as its location and magnitude. The JMA utilizes a database of possible tsunamis due to various earthquake mechanisms for the quick issuance of tsunami alerts. The JMA later revises the issuance process based on the observed tsunami at the coast and the offshore monitoring apparatus.[2]

Thus, techniques for monitoring tsunamis are very important. Installation of coastal tide gauges at ports is an authentic way of monitoring tsunamis. However, tide gauges cannot be used to monitor tsunamis before their arrival at the coast. Offshore tsunami monitoring is necessary to facilitate the evacuation of people near the coast.

Most offshore systems continue to use pressure sensors. The Pacific Marine Environmental Laboratory of the National Oceanic and Atmospheric Administration (NOAA) in the U.S.A. established and has been operating a global distribution of the Deep-ocean Assessment and Reporting of Tsunamis system that uses ocean-bottom pressure sensors and buoys to send data through satellites (for details, see https://nctr.pmel.noaa.gov/Dart/).[3] The stations are installed in the Pacific, Atlantic, and Indian Oceans. In Japan, two pressure sensors were installed offshore of the Pacific coast of the Hokkaido (190–250 km from the coast) and Tohoku (45–75 km from the coast) regions using ocean-bottom cables; records as large as 1 cm or smaller were used for the investigation of tsunamis caused by nearby earthquakes.[4,5] A large tsunami of approximately 5 m height was detected at the ocean-bottom cables placed in the Tohoku region due to the 2011 Tohoku-oki earthquake.[6] After the 2011 Tohoku-oki earthquake, a large national ocean-bottom array of seismograms and pressure sensors were established along the Pacific coast of the Japanese Islands and was named S-net (Seafloor Observation Network for Earthquakes and Tsunamis along the Japan Trench). The network uses ocean-bottom cables of 5,500 km and consists of 150 sites of seismometers and pressure sensors (the network was integrated to the nationwide seismic array called Monitoring of Waves on Land and Seafloor

[MOWLAS]; for details, see https://www.bosai.go. jp/e/).

Additionally, ultrasonic sensors have been used to detect sea wave heights for the Nationwide Ocean Wave information network for Ports and HArbourS (NOWPHAS) operated by the Port and Airport Research Institute of the National Institute of Maritime, Port and Aviation Technology of Japan. The system monitors the wind wave height and can be used to monitor tsunamis. NOWPHAS sensors require that the distance from the coast be less than 10 km in shallow areas with depths of less than 50 m, considering maintenance (for details, see https:// www.mlit.go.jp/kowan/nowphas/index_eng.html).

In contrast to these pressure sensors, a global navigation satellite system (GNSS) buoy would be one of such offshore sensors for detecting tsunamis before its arrival to the coast. The development of the GNSS buoy began in 1996.[7,8] In contrast to pressure sensors that measure sea level change indirectly and require a conversion coefficient, GNSS measures changes in sea level height directly, which is meritorious relative to pressure sensors as it does not require a calibration process. Pressure sensors typically have a small but significant drift, which does not affect instant displacements such as earthquakes or tsunamis, but long-term drift may cause false recognition of seafloor vertical displacement. Moreover, for the detection of tsunamis, GNSS buoys can instantly detect sea surface changes if they are placed within a tsunami source region, while pressure sensors cannot detect changes in sea surface height as the water column height above these sensors placed at the sea bottom does not change its length because the water is incompressible. However, a pressure sensor has a much higher sensitivity at the millimeter-level scale for detecting a change in height compared with a GNSS, which is less sensitive and has a scale of a few centimeters or worse for detecting a change in height. These two types of sensors have complementary characteristics for detecting changes in sea-surface height.

This article briefly reviews the history of the development of the GNSS buoy system and its use in detecting tsunamis. GPS buoys have been used in different applications. A GPS buoy was once used to calibrate the TOPography EXperiment (TOPEX)/ Poseidon satellite radar altimeter.[9] The GNSS buoy system for monitoring tsunamis was also introduced in Indonesia.[10] However, these buoys were lost after a few years because of some unknown reasons. To the best of our knowledge, the development of a

GNSS buoy for tsunami monitoring introduced in this article is a unique project.

Finally, we will discuss how GNSS data obtained from the buoy can be utilized for other applications such as atmospheric and ionospheric research. Land-based GNSS observations have already been applied to these types of studies. For example, the Japanese GNSS nationwide continuous observation network, also called the GNSS Earth Observation Network System (GEONET), which is operated by the Geospatial Information Authority of Japan (GSI), consists of approximately 1,300 sites that have been extensively used for atmospheric and ionospheric research. However, if the present GNSS buoy project goes forward, the GNSS data obtained from the buoy can also be utilized for atmospheric and ionospheric research along with the data collected on land. As the GNSS continuous observation network over the globe has been mostly limited to land thus far, the establishment of a GNSS buoy array in the open ocean will fill the wide gap of continuous GNSS networks over the Earth's surface. This will be discussed in Section 10. In addition, a new attempt to apply a GNSS buoy for the crustal deformation occurring at the ocean floor has been done in our recent experiment, and it will be discussed in Sections 7 and 9.

2. Early developments of the GNSS buoy system

A GNSS buoy was called a GPS buoy in its early stage of development. Figure 1 shows the system: the GPS signal transmitted from the GPS satellite is received at the GPS receiver placed on the board of the buoy. The dual signals (L1 and L2 phases) of GPS are then transmitted to the land base. Another GPS receiver placed at the land base station receives the same GPS signals simultaneously, and the signals on land are compared with those sent from the buoy. As the phase differences between the two signals at the land base and the buoy are a function of the relative position between the two, the position of the buoy can be estimated relative to the position of the land base station. This technique is called the real-time kinematic (RTK) algorithm, which can monitor the position of the buoy relative to the position of the ground base station in real time.

One limitation of this technique is that the maximum distance between the buoy and the base station along the coast for assuring a few centimeters of accuracy would be less than 20 km. Although the noise contamination along the signal path from the
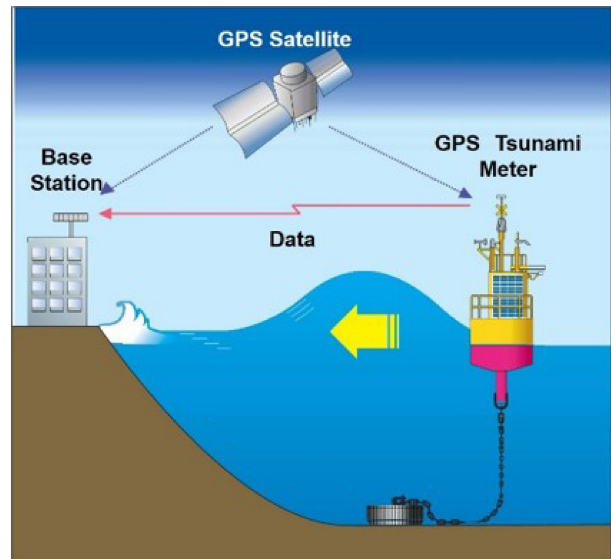

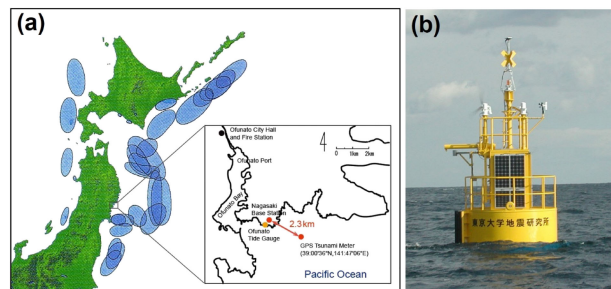Fig. 1.   (Color online) Principle of GNSS buoy for measuring tsunami.[11]

Fig. 2.   (Color online) (a) Location of GNSS buoy experiment off Ofunato City, Northeast Japan. The map with hypocentral regions of large earthquakes (shown in blue) is taken from The Headquarter of Earthquake Research Promotion (1999).[12] (b) Picture of the GNSS buoy off Ofunato City, Northeast Japan.[13]

satellite to the ground station can be canceled by considering the signal differences, the noise cannot be canceled as the distance between the two antennas increases. Consequently, the estimation error of the relative position between the buoy and the land base increases as the distance of the buoy is farther from the base station.

After a few preliminary short-period experiments[7),8)] the first long-term experiment was conducted off Ofunato City, along the Sanriku Coast, northeastern Japan (Fig. 2). The buoy was placed approximately 2.3 km from the land base station, and the experiment was conducted from January 2001 to January 2004.
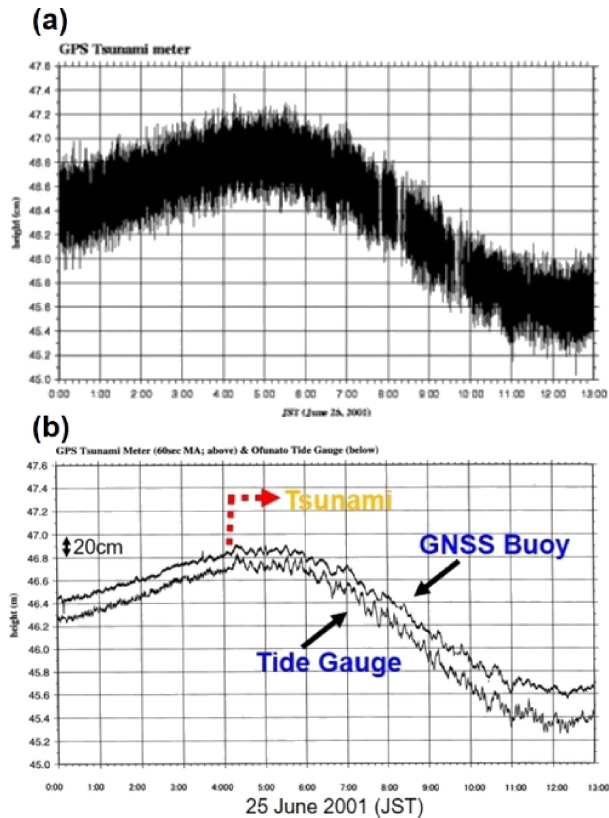
(a)

(b)

Fig. 3. (Color online) (a) Data obtained on June 25, 2001, that include tsunami caused by the South Peru earthquake. (b) Filtered GNSS record from Fig. 3a (above) and the tide gauge record at Ofunato (below).[13),14)]
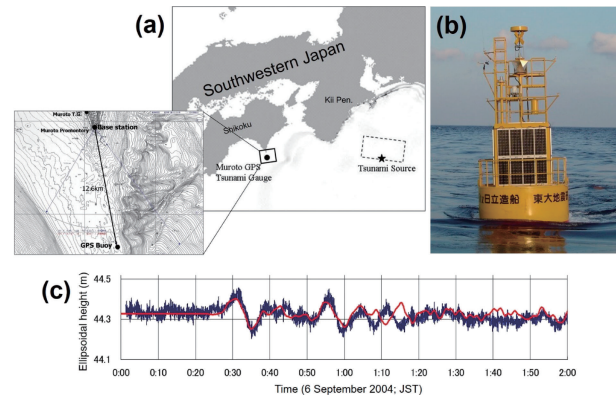
(a) **(b)**

(c)

Fig. 4. (a) Location of the experiment off Cape Muroto and the source region of the 2004 Kii Hanto-oki earthquake, (b) picture of the buoy, and (c) low-pass-filtered record of the GNSS buoy on September 6, 2004 (blue), and the simulated record (red).[11)]

Figure 3 presents the first tsunami data obtained during the experiment. The data were collected approximately 1 day after the 2001 southern Peru earthquake (Mw8.4).[14)] Figure 3a shows a plot of the vertical position of the GNSS receiver equipped on the buoy. The figure shows 13 h of data with 1-s sampling interval. The original record includes high-frequency vertical motion of the buoy due to the wind waves, which often have an amplitude larger than that of the tsunami. However, as the tsunami has a longer period of longer than 10 min or even longer than 1 h, the effects of high-frequency wind waves can be easily filtered out by applying a high-cut filter. We used a moving average method with 60 s of data length on the original record of position. Figure 3b shows that the high-frequency components were filtered out. The figure also includes the record of a nearby tide gauge at Ofunato, located approximately 2 km from the buoy, and shows that the record clearly shows the effect of the tsunami at and after approximately 04:00 JST. Although the

height of the tsunami was only 10 cm above the regular sea-surface height, the tsunami waveform could be easily recognized. This suggests that the precision of the vertical coordinates of the buoy is estimated to be several centimeters. The Ofunato buoy was also able to detect a tsunami with an amplitude of approximately 10 cm caused by the 2003 Tokachi Oki earthquake (Mw7.9).

After this successful experiment, another buoy was placed offshore Cape Muroto, southwestern Japan, for the period of 2004–2006. In this experiment, the buoy was set approximately 13 km south of the tip of the peninsula (Fig. 4a), and another tsunami caused by the 2004 Kii-Hanto Oki earthquake (Mw7.3) was observed.[11)] The experiment aimed to disseminate observed data to the public through the Internet. The obtained data were separated into two terms: long- and short-wavelength data that might include tsunamis and wind waves, respectively. The latter is important not for tsunamis but rather for daily monitoring of offshore wave heights. This is especially useful for daily life activities, such as those of fishery people, to monitor wave heights offshore. As tsunamis are highly rare, wave monitoring tools are especially welcomed by coastal residents and fishermen.

Another examination was conducted to determine how the obtained record matches the simulated record. Figure 4c shows that both records are consistent, suggesting that the observed tsunami record can be used to estimate the characteristics of the tsunami source. Conversely, it was found that the tsunami generated by the 2010 Chile earthquake (Mw8.8) occurred 26 min after the simulated tsuna-

mi.[15] The difference in the arrival time for the distant tsunami was investigated, and it was suggested that the effects of compression and dilatation of seawater, elastic tsunami loadings on the solid Earth, and the geopotential variations associated with the motion of mass during tsunami propagation were responsible for the travel time delays.[16]

After these successful experiments, the GNSS buoy was adopted as part of the NOWPHAS. The NOWPHAS is aimed at monitoring offshore wind waves for fisheries and other coastal industries, and the buoy is called "GPS wave meter", though it is also used for monitoring tsunami. The first operational buoys in NOWPHAS were installed offshore in southern Iwate Prefecture and central Miyagi Prefecture.[17] These regions are along the Sanriku Coast of Japan, where the tsunami risk is high.

Because of the technical limitations of the RTK method described above, the GNSS buoys for NOWPHAS have been deployed within 20 km from the coast. This distance from the coast maintains a lead time of approximately 10 min for tsunami arrival at the nearest coast. From the disaster mitigation perspective, determining how quickly the alert can be issued after the detection of tsunami arrival at the buoy is important.

The data of NOWPHAS are disseminated through webpages in real time. In 2008, the JMA decided to monitor the NOWPHAS buoy data and since then have used these data to provide people with tsunami information in their tsunami alert.

3. The 2011 Tohoku-oki earthquake

The Port and Airport Research Institute deployed 15 GNSS buoys around the Japanese Islands for NOWPHAS before the 2011 Tohoku-oki earthquake (Fig. 5). Seven sites were located offshore of the Sanriku coast, considering that the area has historically been a risky area for tsunami disasters.

A few minutes after the mainshock of the Tohoku-oki earthquake occurred at 14:46 JST of March 11, 2011, the JMA issued the first tsunami alert using their predetermined procedure.[2] However, the issued alert indicated that the tsunami heights would be 6 m along the Miyagi Prefecture coast and 3 m along Iwate Prefecture. These were significantly smaller than the resultant tsunami, which was higher than 10 m, along these coasts. The estimation was small because of the under-estimated magnitude of the earthquake. This occurred because many seismograms for earthquake
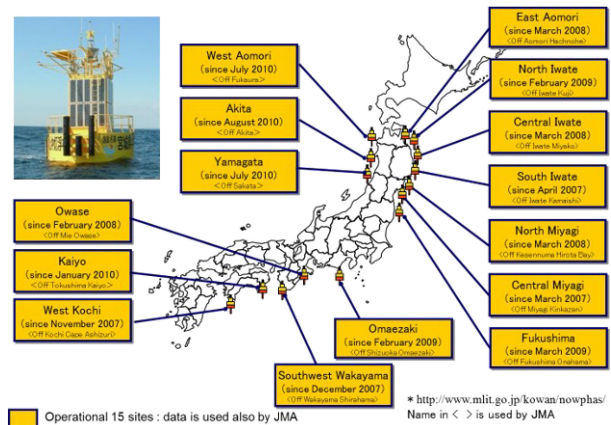

Fig. 5. (Color online) GNSS buoy established before the 2011 Tohoku-oki earthquake by NOWPHAS. Modified from Terada et al. (2011).[13]

early warning alerts were clipped instrumentally, as the ground shaking intensity was much larger than the instrumental limit.[2]

A JMA staff who was monitoring the NOWPHAS records recognized that a GNSS buoy showed an acute sea-level rise of more than a few meters and judged that the tsunami would be much larger than the height of the first tsunami alert, knowing that the tsunami at a far offshore magnifies toward the shallower part of the coast and thus would be several times larger than that at the far offshore. The JMA revised the height in the tsunami alert along the Sanriku coast from 6 m to more than 10 m in Miyagi at 15:14 JST.[2] Just after its revision, the first tsunami arrived at the Sanriku coast. However, the alert was received too late, and the tsunami claimed more than 18,000 lives.

Figure 6 shows the records of tsunamis taken at three NOWPHAS sites along the Sanriku coast.[13),18] The sites near the epicentral area stopped sending the data to the server immediately after the maximum height of the tsunami was recorded at the buoy. This occurred because of malfunction of the data communication link or because of either the unavailability of the Internet or the loss of power after the earthquake. However, the recording was continued at the site with the use of a backup battery, and the obtained coordinates were stored in the storage at the sites even after the failure, so that the record could be recovered afterwards, as shown in Fig. 6.

4. Lessons from the Tohoku-oki earthquake

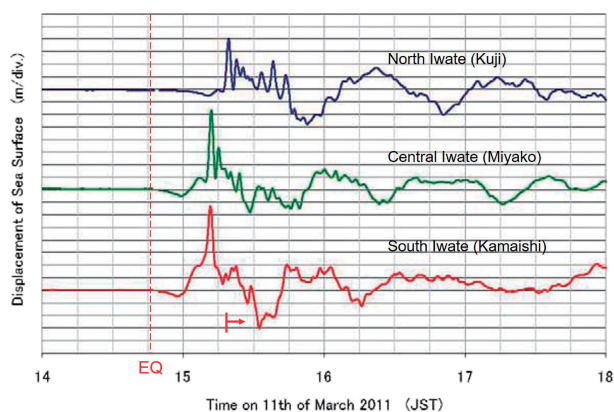The lead time of approximately 10 min from the

Fig. 6. Recovered records of tsunami data from the 2011 Tohoku-oki earthquake. EQ is the time of the earthquake. The red arrow roughly shows the timing of the tsunami arrival.[13]

detection of the tsunami at the buoy to the arrival of the tsunami to the coast was too short to facilitate evacuation. Extending the lead time requires buoy deployments much farther from the coast. Although there is no linear relationship between the distance to the coast and the lead time, farther deployments of buoy to, for example, 50 km or more than 100 km, will substantially improve the lead time.

The amplitude of the tsunami decreasing with the water depth is a disadvantage of placing a buoy far from the coast. Contrarily, the height of the tsunami far offshore would be amplified a few times as it approaches the coast. Although this may not be troublesome considering that a hazardous tsunami may be tens of centimeters in height even at a deep ocean, an accuracy of few centimeters would still be one of the requirements for measuring sea-level changes accurately.

5. New developments of the GNSS buoy after the Tohoku-oki earthquake

Considering the lessons from the 2011 Tohoku-oki earthquake and tsunami, we designed a new GNSS buoy to overcome the problems that the old system showed during the Tohoku-oki earthquake. The required specification of the buoy is to deploy it farther offshore from the coast. Because the new developments have already been documented in our previous paper,[19] we briefly review the new system and present our recent results from this new system.

5.1. Introduction of the PPP-AR algorithm. Considering that a distance limitation of less than 20 km is required when the RTK algorithm in our old system is used, we had to introduce a better algorithm for positioning the buoy far offshore. For this purpose, we employed a new algorithm called precise point positioning with ambiguity resolution (PPP-AR) or PPP-RTK.[20),21)] As PPP-AR uses a single point positioning algorithm, it does not require the base station on land to make a baseline. The precise point positioning (PPP) approach has been widely used for crustal deformation research since around 2000.[22)] Although it is a convenient positioning method, it is necessary to use precise orbits and satellite clock information, estimated from integrated analysis using global data, which can be available only a few weeks after the observation. Therefore, PPP was limited to offline analysis during its early stages of development. However, recent developments in rapid data analysis and communication technologies have allowed us to obtain precise orbits and clocks in real time. This allowed us to introduce the PPP algorithm for buoy positioning. There are two ways to use PPP, with or without fixing ambiguity, inherent in using the phase of the GNSS signal for positioning analysis. We used PPP-AR as it provides us with better resolution and accuracy.[21)] We used commercial software called RT-Net, which was developed based on the PPP-AR algorithm.

As PPP-AR requires precise orbits and clocks in real time on the buoy for real-time monitoring, the information should be sent to the buoy in real time. For this purpose, we first obtained the necessary information through the Hitz Data Center operated by the Hitachi Zosen Corporation, where GEONET data are used to obtain precise orbits and clocks in real time.

Hitachi Zosen Co. examined the accuracy of PPP-AR using GEONET data. The coordinates of the Shimokawa GEONET site were estimated using the precise orbits and clocks generated by three regional networks of GEONET for distances of 150, 1,000 and 1,500 km. Figure 7 shows the results. The three coordinate components (N–S, E–W, and up) were estimated during 9 days of data acquisition, and short-term variability was obtained for each component. Although the vertical component, which is important for tsunami detection, is less precise than the horizontal components, the standard deviation (SD) for 1,500 km is still less than 30 mm. Therefore, PPP-AR may have a high enough precision to detect significant tsunamis greater than a few centimeters at locations far from the Japanese Islands.

5.2. Introduction of satellite telemetry. We employed a satellite data transmission system for data telemetry. Until the Tohoku-oki earthquake in 2011, a GNSS buoy system such as NOWPHAS, used
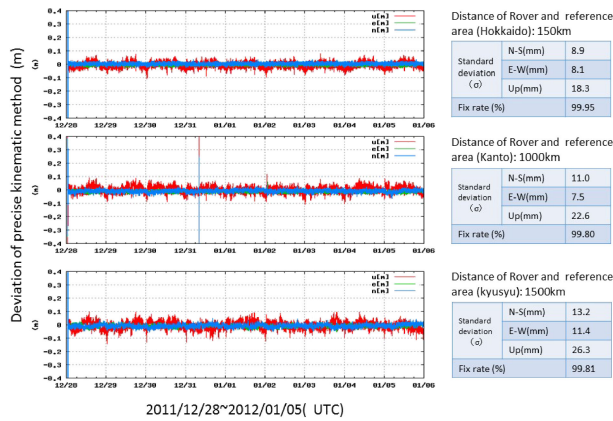
Distance of Rover and reference area (Hokkaido): 150 km		
Standard deviation (σ)	N-S(mm)	8.9
	E-W(mm)	8.1
	Up(mm)	18.3
Fix rate (%)		99.95

Distance of Rover and reference area (Kanto): 1000 km		
Standard deviation (σ)	N-S(mm)	11.0
	E-W(mm)	7.5
	Up(mm)	22.6
Fix rate (%)		99.80

Distance of Rover and reference area (kyusyu): 1500 km		
Standard deviation (σ)	N-S(mm)	13.2
	E-W(mm)	11.4
	Up(mm)	26.3
Fix rate (%)		99.81

Fig. 7. (Color online) Results of PPP-AR at the Shimokawa GEONET site for different distances of reference networks that generate precise orbits and clocks: (top) 150 km, (middle) 1,000 km, and (bottom) 1,500 km. The observation period is from December 28, 2011, to January 5, 2012. Courtesy of Hitachi Zosen Co. 2012.

a marine radio system as the distance between land and the buoy was less than 20 km. As the distance exceeds 20 km, land-based radio systems get less reliable to use because the buoy cannot be seen from land owing to the Earth's sphericity. Therefore, using satellite telemetry is mandatory if the GNSS buoy is placed farther than 20 km.

If we apply the PPP-AR algorithm, the distance from land to the buoy can be 1,000 km or more from the Japanese coasts, if the precise orbits and clocks are obtained from the GEONET regional array. Thus, if precise orbits and clocks can be obtained through the satellite system, the position of the buoy can be anywhere in the ocean.

As a preliminary experiment for satellite telemetry systems, we first used the Japanese Engineering Test Satellite VIII (ETS-VIII) and the Quazi-Zenith Satellite System (QZSS, also known as Michibiki), a Japanese GNSS satellite. The buoy used in our experiment was operated off from Muroto. The system is shown in Fig. 8. First, the precise orbits and clock parameters were generated by the Hitz Data Center utilizing real-time obtained GEONET 1 Hz data. These orbits and clocks were transmitted through the Michibiki satellite to the buoy. The GNSS phase data obtained on the board of the buoy were analyzed using telemetered precise orbits and clocks. The resultant position of the buoy was then sent back to the land base using ETS-VIII, and the data were visualized on the web and disseminated to users.

6. Field test experiments for the new system (2013–2016)

To test the new PPP-AR algorithm and satellite telemetry in the ocean, we conducted a series of field experiments from December 16, 2013, to January 5, 2014, and from June 1, 2014, to June 21, 2014. We borrowed one of the fishery buoys operated by Kochi Prefecture, Japan. Kochi Prefecture operates a number of fishery buoys, including Kuroshio Bokujyo (Kuroshio Ranch, or Kuroboku for short), offshore of Kochi Prefecture, as some species of migratory fish tend to come around floating materials such as buoys, which help fishermen to catch these fishes easily. We borrowed the Kuroboku No. 16 buoy. The buoy is located approximately 35 km south of Cape Muroto, Kochi (Figs. 9a and 9b). The GNSS antenna was set at the top of the pillar at the center of the buoy. A simple flat omnidirectional plane antenna was used for satellite data transmission, considering the buoy rotation and tilt. Other ancillary pieces of equipment were placed on the buoy deck. Solar panels and batteries were used as the power supplies. The GNSS receiver was sampled every second. The precise orbits and clocks necessary for data analysis on the buoy were provided through the LEX signal of the Michibiki satellite. The coordinates obtained every second were transmitted to land through the ETS-VIII satellite. The coordinates were forwarded to the web server placed at Kochi National College for dissemination.

Figure 9c shows the 2 days of data obtained from the experiment. Data of 1 Hz for 33 h from June 18, 2014, to June 19, 2014, are shown. Figure 9c (top) shows high-pass-filtered data together with tidal component data, and Fig. 9c (bottom) shows low-pass filtered data. If a tsunami is recorded, it will appear in Fig. 9c (bottom). It should be noted that occasional data gaps are minor problems in the time series, where data transmission is interrupted. The unstable communication link between the buoy and the satellite due to the tilting of the buoy could be a potential reason. Figure 10 shows a comparison between the transmission rates and the significant wave height. The upper plot shows the transmission rates for which the scale is shown on the left, and the lower plot is the significant wave height for which the scale is shown on the right. The transmission rates decrease as the significant wave heights increase. This suggests that the tilt of the buoy due to high waves reduces the gain in the satellite direction of the
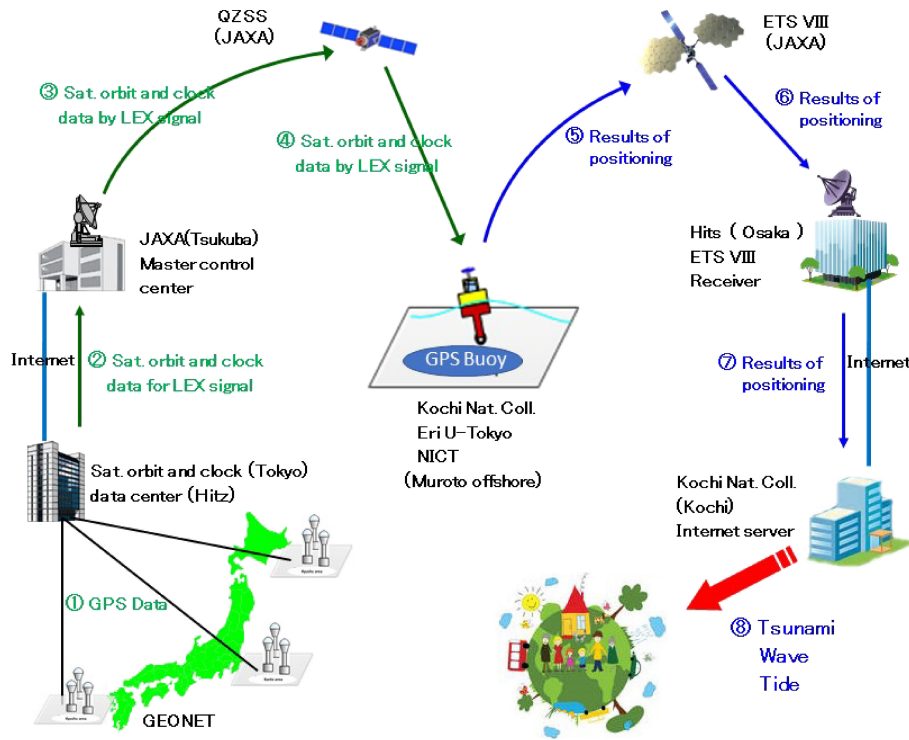
Fig. 8. (Color online) System design for the data acquisition, analysis, and dissemination using two satellites: ETS-VIII and QZSS.[23]
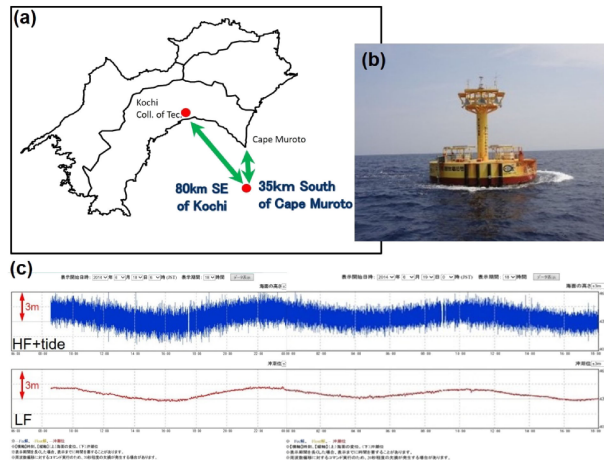

Fig. 9. (Color online) (a) Location of the buoy and Kochi National College, where a data server is placed, (b) Kuroboku No. 16 buoy used for the experiment, and (c) a part of the obtained data.[24]

Fig. 10. (Color online) Comparison of data transmission rates and significant wave height.[24]

antenna for satellite communication mounted on the buoy.[25]

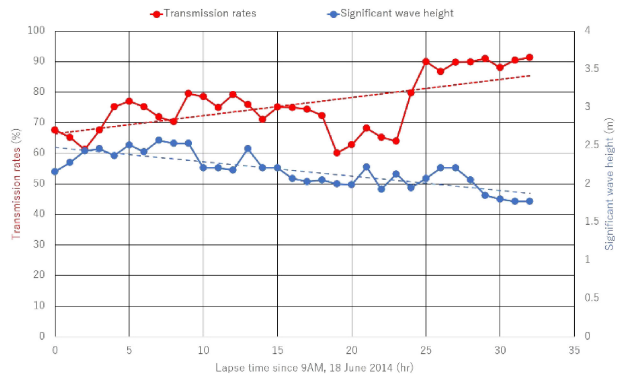Considering that some data were missing, we conducted another experiment on December 8–10, 2015. As the antenna tilt is suspected to be the cause of data failure, we employed a gimbal mechanism that stabilizes the tilting of the antenna on the board of the buoy. A simple gimbal apparatus carrying the plane antenna was devised (Fig. 11). Two antennas were placed on the same vessel for comparison: one was placed on the gimbal apparatus, and the other was fixed to the deck. Two vessels, Yuge-maru, the school ship of Yuge College of 240 tons, and Hamakaze, another small school boat (see Fig. 12), were used to compare the data.
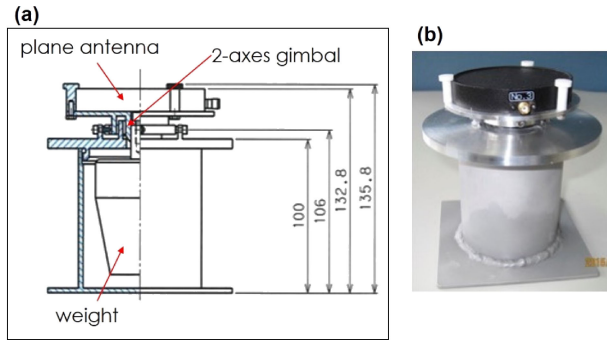
Fig. 11. (Color online) (a) Design of the gimbal for supporting a plane antenna. Unit: mm. (b) Picture of the gimbal and the plane antenna.[24]

Fig. 12. (Color online) (top) Yuge-maru and (bottom) Hamakaze, both operated by Yuge College.[24]
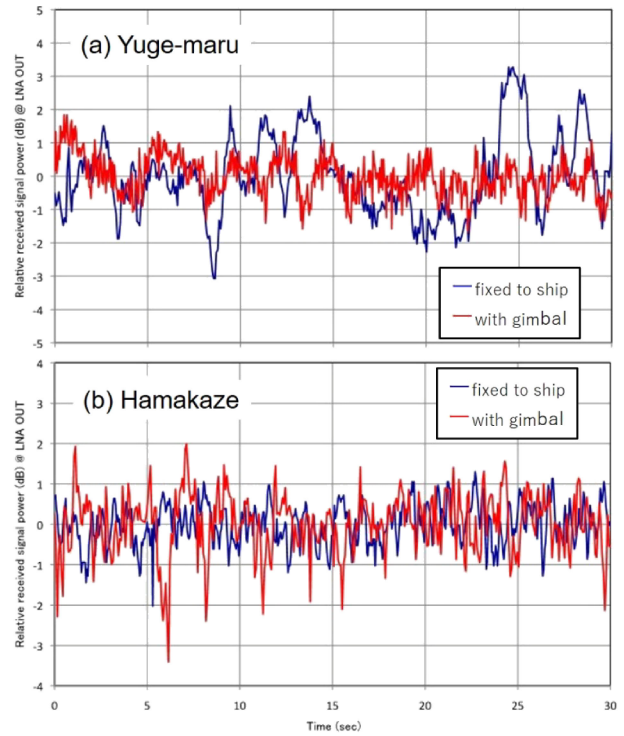

Fig. 13. (Color online) Comparison of received signal power with a gimbal apparatus (red) and without it (blue), for the case of (a) Yuge-maru and (b) Hamakaze.[24]

Figure 13 shows a part of the results comparing the signal power received from the satellite.[24],[26] Figure 13a is for the Yuge-maru, and Fig. 13b is for Hamakaze, the red line shows the case with the gimbal apparatus, the blue line shows the case without it, and the antenna was fixed to the deck of the ship. The case with the gimbal apparatus in Fig. 13a, the case for Yuge-maru, shows a significant reduction in fluctuation owing to the usage of the gimbal apparatus. However, Fig. 13b, which used Hamakaze, does not show any significant reduction in the fluctuation of the received signal power. Because the sizes of the two ships were different, the different results might be due to the different characteristics of the ship sway period.

In the ocean, tilting oscillation of the buoy at the sea surface changes the antenna gain. Therefore, knowledge of the radio propagation characteristics due to the tilting oscillation for the satellite communication link is very important for the future development of the system. Hence, developing a radio propagation model for signal transmission between the sea surface and the satellite based on the data obtained from the ocean is necessary. We conducted another experiment on August 25–26, 2016, in Hiuchi-Nada of the Seto Inland Sea, Southwest Japan. In the experiment, Yuge-maru was used as the floating body in the ocean, and two plane antennas, one fixed to the ship and the other placed on the gimbal, were used again, together with a gimbal. A tilt meter and GNSS were also used to measure tilt oscillation and ship position. The results from the obtained data suggest that the change in

the strength of the signal can be expressed as the summation of the deterministic and stochastic parts, for which the former part is due to the change in antenna gain owing to the tilting of the antenna and the latter part can be shown as a log-normal distribution.[27] These results will be considered to design a new buoy system in the future.

7. A new challenge for the ocean floor crustal deformation measurement

Monitoring of ocean floor crustal deformation based on the combined use of acoustic ranging and GNSS positioning has been a recent challenge in earthquake observation. This idea was first published by a U.S. researcher in 1985,[28] but later the technology was developed mainly by Japanese researchers.[29]–[32] The technique, called the GNSS-Acoustic (or simply GNSS-A) system, for ocean floor positioning is such that the acoustic ranging from the transducer, attached to the vessel, to the ocean floor transponders is used for estimating the position of the centroid of the geometry of the array of transponders and the position of the vessel is estimated by GNSS (Fig. 14). The position of the centroid of the array geometry at the ocean floor can be estimated with an accuracy of a few centimeters. Repeated measurements of the position of the centroid of the geometry can provide information on the crustal movement of the ocean floor.

This method has led to a new understanding of crustal movements at the ocean floor, for example, the motions of plates or blocks,[33]–[36] plate convergence and interplate coupling,[37]–[48] co-seismic displacements,[49]–[51] and post-seismic deformations.[52]–[56] Its unprecedented magnificent result was shown during

the 2011 Tohoku-oki earthquake,[57] in that displacements larger than 30 m were observed at the ocean floor near the epicenter, and the results were used for precise estimation of earthquake slip distribution.[58] Thus, the GNSS-Acoustic technique has become one of the most important tools for monitoring ocean floor displacements and even for providing unprecedented important information on understanding the coupling mechanism of subducting oceanic plates against the overriding plate and the mechanisms of interplate earthquakes that occur along their boundaries.

One problem with the current GNSS-Acoustic system is that the system uses a vessel for GNSS positioning, so that the measurements are not continuous but are in limited numbers annually. The Japan Coast Guard largely oversees observation, using a survey vessel for GNSS-Acoustic observation. This method limits the observation frequency to several times annually at a site. Although the frequency is enough to delineate steady plate motion, it may not be enough for finding important short-term events such as slow slip events for a few weeks or shorter. In order to establish frequent observations, one possibility would be to use our GNSS buoy instead of a vessel for the GNSS-Acoustic system.

In addition to using PPP-AR and satellite data transmission for the GNSS buoy in our new experiment, we incorporated the challenge of observing the ocean-bottom crustal movement in our next experiment on the GNSS buoy. A similar buoy system for GNSS-A was developed by another research group, who used a loosely moored buoy.[59]–[61] Other researchers have evaluated the use of the Wave Glider (Liquid Robotics, Inc., Sunnyvale, CA 94089, U.S.A.) as a novel platform for GNSS and acoustic measurements.[62]–[65]

Although the principle is similar, continuous measurements using a buoy instead of a vessel require some technical developments. First, the signals sent and received at the transponder attached to the buoy should be picked automatically and precisely. Sometimes, the received signal is contaminated by various noises, especially by the reflected waves from the buoy itself and/or the sea surface. We developed an algorithm to select the correct arrival time of the direct signal. Test experiments of the algorithm, conducted in the buoy experiments in June and September 2017, showed that the automatic algorithm judged with 99.5% success for the correct signal and rejected 90.9% success for the incorrect signal, considering the visual decision is true.[66] Second, to estimate the travel time of the acoustic
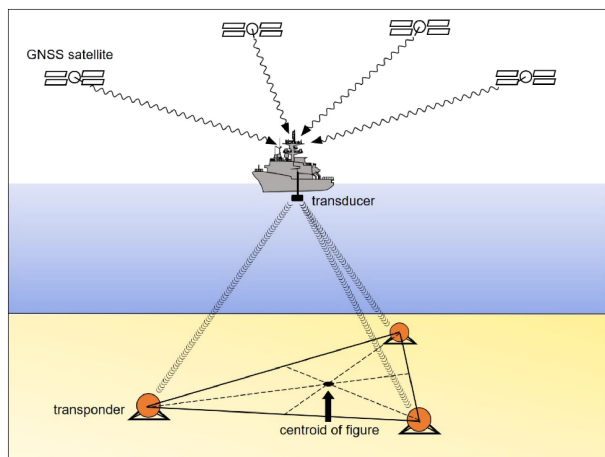
Fig. 14. (Color online) Concept of the GNSS-Acoustic system.

signal between the transponder and the transducer precisely, the distribution of acoustic velocity along the travel path should be precisely known. Although a simple model based on the vertical profile of conductivity and temperature could be used, it was asserted that the introduction of the horizontal gradient estimation of the acoustic velocity is necessary to improve the precision of position estimation of the ocean floor.[67] As it is difficult to make conductivity, temperature, and depth (CTD) observations in each acoustic ranging, as can be performed for a vessel observation, we decided to estimate the horizontal gradient together with the position of the transponder array. The horizontal gradient is introduced as an unknown parameter because the horizontal gradient and the position of the array are in a trade-off relationship. The estimation of these parameters simultaneously requires that the buoy widely move around the array area. However, as we cannot control the position of the buoy, it is sometimes difficult to precisely estimate the horizontal gradient, which results in a large position error of the array.

We then decided to make the process slightly different. First, we precisely estimated the array configuration by using a vessel. Then, assuming that the configuration does not change from time to time, the position of the ocean floor is estimated by the summation of the predetermined array position and the time-variable displacement of the array.

To precisely estimate the array configuration, we used six acoustic and CTD observations between June 2017 and June 2019 using a vessel. From these observations, we estimated the array positions by the least square method so that the root-mean-square (RMS) between the observed travel times and theoretical travel times becomes minimum.[68] The results showed that the RMS of estimating the horizontal gradient of the sound speed was 0.04–0.06 among the six observations (Tables 1 and 2), suggesting that the array position is estimated with an accuracy of approximately 5 cm.

Finally, based on these results, we decided to use a grid search method to estimate the change in the position of the array from the travel time observations.

8. The new GNSS buoy system experiment (2016–2021)

Figure 15 shows the system design for the new experiment that started in November 2016. As neither the ETS-VIII nor Michibiki was available

Table 1. Estimated position of the ocean bottom array

	Latitude	Longitude	Ellipsoidal height (m)
Unit 1	32.485288131°N	133.199879448°E	−756.814
Unit 2	32.493409868°N	133.211624751°E	−748.868
Unit 3	32.481173867°N	133.213997997°E	−762.598

Table 2. Estimated results of the horizontal gradient of sound speed

Date (yyyy-mm-dd)	ΔV (m/s/km)	ϕ (°)	RMS (ms)
2017-06-06	0.27	121	0.04
2017-06-09	0.21	136	0.05
2018-05-31	0.14	200	0.06
2018-06-01	0.11	184	0.05
2019-06-04	0.18	174	0.06
2019-06-05	0.16	164	0.05

for the experiment, we employed a commercially available satellite called Thuraya for data transmission between the buoy and the ground base. We borrowed the Kuroboku No. 18 buoy from Kochi Prefecture. This buoy is located approximately 32 km south of the Cape Ashizuri (Fig. 16).

We set the ground base station at Niyodogawa-cho in Kochi Prefecture, and a server to operate the system was set at this base (Fig. 16). The precise orbits and clocks for PPP-AR were generated at the Hitz Data Center and sent to the Niyodogawa base, and the data were transmitted from the base to the buoy through the Thuraya satellite.

The GNSS data obtained on the board of the buoy were analyzed using PPP-AR. We also used the point precise variance detection (PVD) positioning algorithm.[69] This method uses the received carrier phase signal of GNSS and estimates the change in antenna position using the phase change. As it does not estimate the absolute coordinates of the antenna position but only estimates the "change" of position occasionally, we do not require fixing integer ambiguity of the line-of-site length between the satellite and the antenna; the results are robustly obtained as long as the satellite signal is locked. However, unlike PPP-AR, PVD requires low-cut filtering of the data, which reduces the sensitivity to a long wavelength. Consequently, PVD is effectively used for monitoring wind waves but not long waves such as tsunamis. PVD is effectively used to monitor daily oceanic conditions for fisheries and other ocean
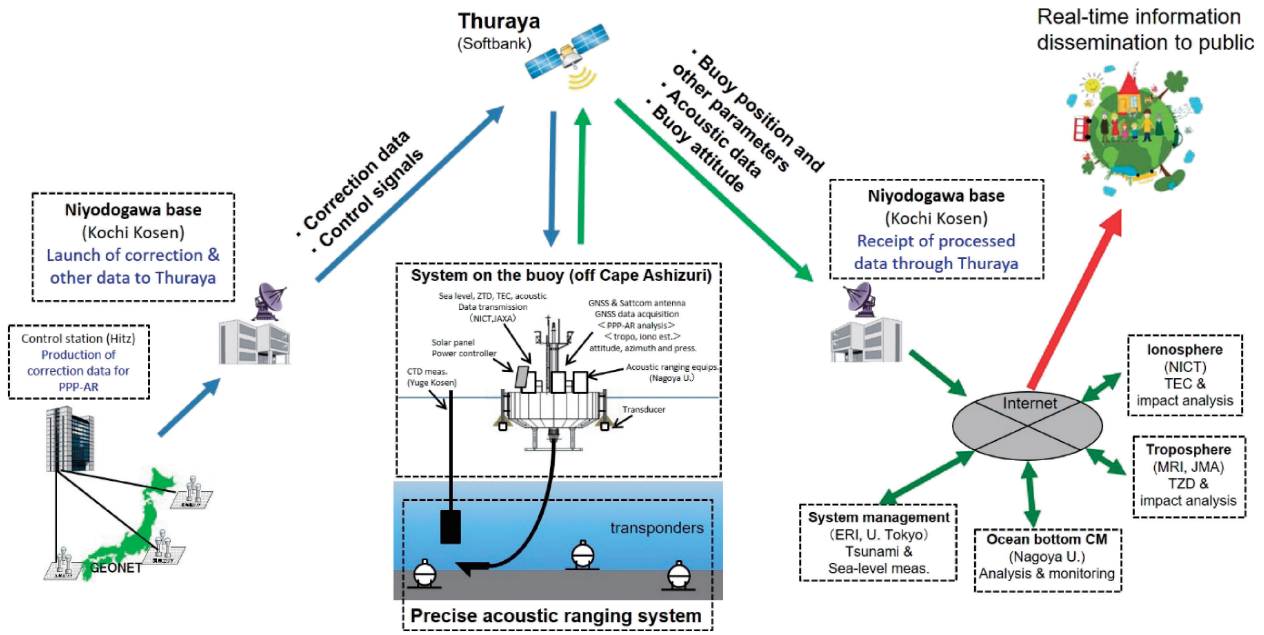
Fig. 15.   System design for the recent experiment from 2016 to 2021.[19]
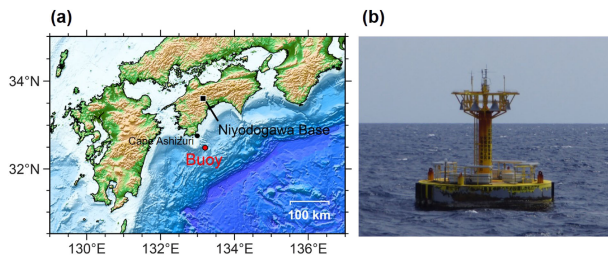

Fig. 16.   (Color online) (a) Locations of (bottom) the buoy used for the experiment and (top) the ground base station in Niyodogawa-cho. Bathymetry data were taken from SRTM30_plus.[70] (b) Buoy No. 18 of the Kuroshio Bokujyo (Kuroboku).[19]
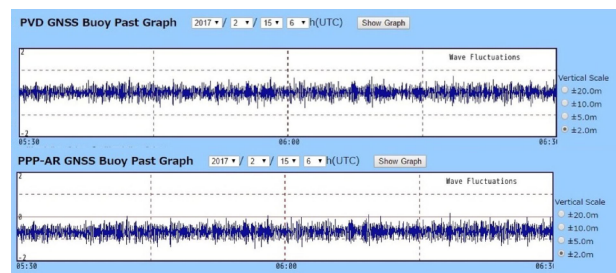

Fig. 17.   (Color online) Sample data of (top) PVD and (bottom) PPP-AR.[19]

activities. Considering that we obtain two kinds of sea surface changes using two algorithms, PPP-AR for long wavelengths and PVD for short wavelengths, the obtained precise position of the buoy is sent back to the base through the same satellite.

The system was first established in November 2016, and the experiment continued until February 2021. Figure 17 shows the sample data of the estimated vertical displacements of the buoy. Figure 17 (top) shows the plot by the PVD method, and Fig. 17 (bottom) shows the plot by the PPP-AR method. For PPP-AR, the daily and sub-daily tidal components were removed. The PPP-AR and PVD records appear the same when the tsunami is excluded. Only when a tsunami is coming can PPP-

AR draw the curve due to the tsunami. These results are expected to be obtained from our previous experiments.

We expected that the system would be continuously used if every part worked well. However, owing to various problems, continuous observations were suspended numerous times during the experiment. It is occasionally difficult to resolve the central cause of such suspension; disruption of power supply on the buoy, malfunction of the PC on the buoy, and suspension of the satellite communication link are all possible causes. For example, we designed a power system consisting of solar panels and batteries, so that sufficient power is generated even if several days of loss of sunshine occur. However, it seems that the generated power was insufficient, and as a result, the system stopped, especially during the winter season

when sunshine decreased. Power generation was estimated assuming that the solar panel was horizontal. However, tilting of the buoy may have decreased the efficiency of power generation. It was suggested that the center pillar at the buoy may create a shade on the panel and reduce the production of electricity.[71] To overcome this problem, we added solar panels in 2019–2020. The breakdown of machines is another major source of data loss. In harsh environments in the outer ocean, some delicate electric parts are always threatened with failure. Additionally, the loss of communication links was a problem. It was difficult to clarify whether the loss of data occurred from the failure of the communication link or malfunction of any part of the buoy. We had to check the data and hardware cautiously for this purpose and had to ask supporting companies to check and adjust the parameters of the system, which was cumbersome and time-consuming. Frequent maintenance trips are thus required to ensure the entire system on the buoy works well. However, the strong current of the Kuroshio and strong winds due to typhoons and low pressures often prevented us from reaching the buoy. These are some of the problems to be solved in future developments of the system.

Figure 18 shows the recorded period of the results for PVD and the daily fixed rates for PPP-AR on the buoy (Fig. 18a), and both records are stored at the Niyodogawa base (Fig. 18b). Although the experiment started in November 2016, it stopped for a short time period and was unable to resume rapidly. The system was restarted in February 2018 after it was redesigned. Figure 18 shows the records since then. As can be seen in the figure, there are periods in which both the buoy and the base have records, but there are also periods in which records either from the buoy or from the base, or both, are missing. In the case of a power failure on the buoy, none of the data can be stored on the buoy or at the base. On the buoy, PVD has recorded data over longer periods of time as it uses a simple algorithm that uses received phase data, whereas PPP-AR requires precise orbits and clocks separately sent from the satellite. Therefore, once the satellite communication link from the land to the buoy has been suspended, PPP-AR cannot be performed on the buoy. Even if the data are stored on the buoy, the data cannot be sent to the land if the satellite communication link is lost, as there is no time of failure at the base station server. There were some cases where the data were stored on the server at
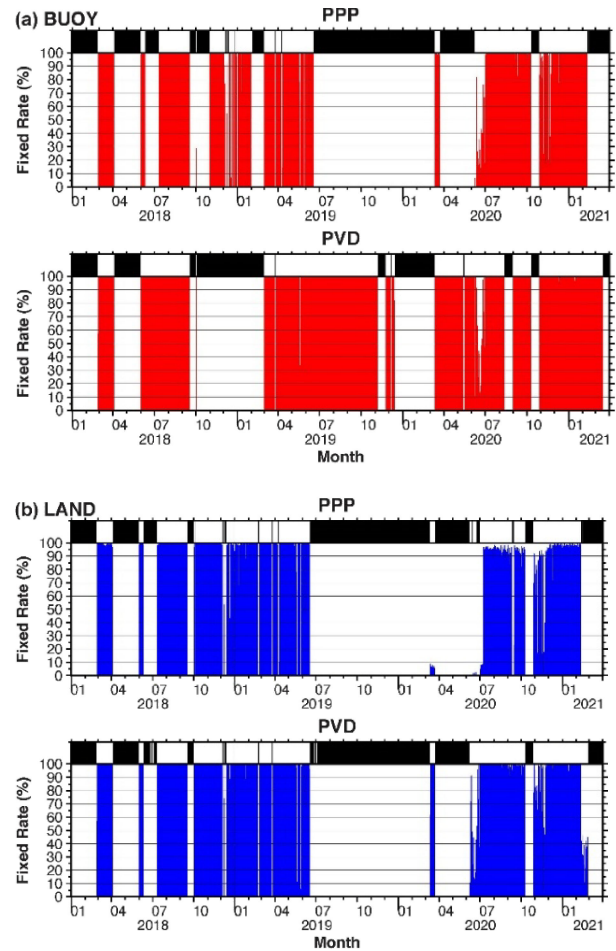

Fig. 18. (Color online) Periods of obtained record of (a) a fixed rate of PPP-AR and PVD record on the buoy and (b) both records that are stored at the Niyodogawa base.

Niyodogawa base, although the data on the buoy were missing, probably because the buoy data were lost from a locally recorded logger. Further examination of these periods of missing data is warranted in future studies.

9. Results of continuous observation of ocean floor crustal movements

Figure 19 shows the data obtained during the period from August 18, 2020, to January 15, 2021. The top three plots (Units 1–3) show the observed travel times from the transducer at the buoy to the three sea-bottom transponders estimated using the algorithm developed by the present project.[71]

The middle three plots represent the positions of the transducer at the buoy. The positions of the transducer until November 25, 2020, were obtained by offline analysis using the PPP algorithm with
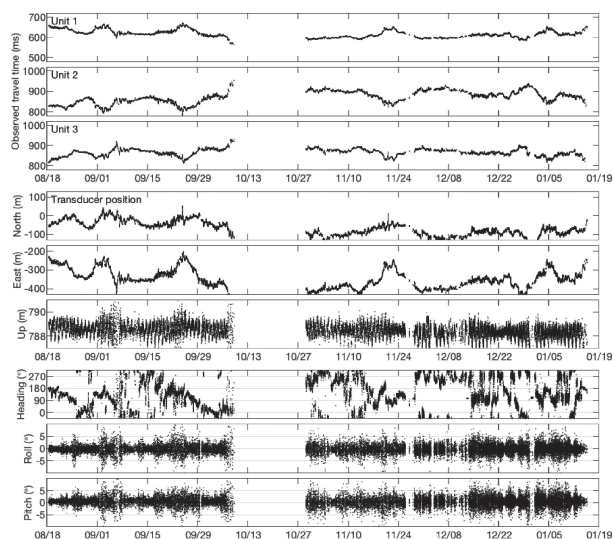
Fig. 19. GNSS-Acoustic observation data from August 18, 2020, to January 15, 2021. (top) Travel times between buoy and transponders (Units 1–3), (middle) Transponder position at the buoy (North, East and Up) and (bottom) direction and tilting angles of the transducer (Heading, Roll and Pitch). Position of the transducer is measured from the centroid of the transponder array geometry. Position was obtained by PPP before November 25, 2020, and PPP-AR after November 26, 2020.

precise orbits and clocks called as MADOCA (Multi-GNSS Advanced Demonstration tool for Orbit and Clock Analysis), which was developed by the Japan Aerospace Exploration Agency (JAXA). The positions after November 26, 2020, were obtained using PPP-AR analyzed on the buoy and sent by the real-time satellite transmission. The position of the transducer was shown by placing the origin of the coordinates at the center of the triangle made by the three transponders at the ocean floor.

The bottom three plots are the heading, roll, and pitch of the buoy measured by a gyro installed on the buoy, assuming that the direction of the transducer attached to the buoy is the direction of the bow.

The height of the GNSS antenna and the tilting (pitch and roll) intermittently showed a large amplitude during the end of August to early October 2010. This is due to the passage of typhoons near the buoy. Because the typhoon passed around October 10, 2010, the GNSS observation stopped because of the GNSS antenna breaking. This was restored on October 28, 2020.

Figure 20 shows the results. The top two plots of the figure are the averaged central positions of the ocean-bottom transponder array. The bottom three plots are the estimated sound speed structure. V_0
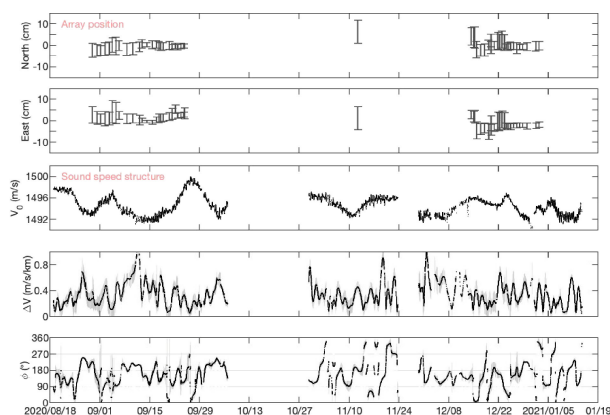

Fig. 20. (Color online) (top) Centroid of the ocean bottom transponder array (North and East) and (below) the analyzed results of the sound speed structure (V_0, ΔV, and ϕ).[72]

is the average sound speed, and ΔV and φ are the horizontal gradients. The position of the center of the array was estimated using data collected over 28 days. The positions in Fig. 19 are plotted in the center of the 28-day time window. The averaged data provide a much smoother change in the position of the transponder array. However, it can be readily seen that there is an acute jump in position around December 14, 2020, which is due to a change in the positioning algorithm from PPP to PPP-AR on November 26. Note that the change in algorithm occurred in order to choose the best method at the time of positioning. The possible areas narrowed by the grid search are shown by vertical bars called the RMS. Figure 21 shows the horizontal plots of the estimated centroid positions of the array. The RMS error of the estimated centroid position of the array was 3.0 cm. This suggests that the position of the ocean floor based on our developed system can be estimated with an accuracy of a few centimeters. This may be the first system to record a continuous change in the position of the ocean floor with such unprecedented accuracy.

In principle, acoustic measurements can be collected and analyzed in a short duration (*i.e.*, less than 1 day). However, in the present experiment, the conditions in which acoustic measurements were obtained were not ideal: 1) the site is in an area where the Kuroshio Current is strong and the temporal change in the spatial gradient of the speed of sound was large, and 2) as the water depth was shallow (approximately 800 m), the temporal change in the speed of sound degrades the accuracy of estimating the position of the array. Therefore, we used a longer dataset consisting of 28 days to average
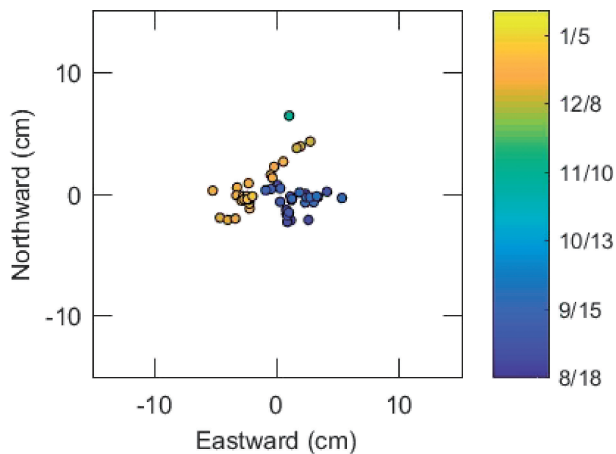
Fig. 21. Centroid of the geometry made by the three transponders at the ocean floor.

out a highly variable sound speed gradient and its temporal change to suppress the temporal variation of the estimated seafloor position. When the length of data was shorter, the variation in the estimated position was larger; for example, if the data length was 14 days, then the SD of the estimated centroid position of the array was larger than 10 cm. If we use the recently proposed method for the estimation of sound speed structure,[73] a better estimation using a shorter data length could be attained, which is being attempted in further studies.

10. Discussion

In our series of GNSS buoy experiments for tsunami monitoring, we showed that it is worth pursuing their development for far offshore operations. However, some operational problems remain to be solved.

First, buoys may have to be operated autonomously. Although maintenance of the buoy is crucial for the long-term operation of the system, it is costly and workers sometimes find it difficult to reach and work on the buoy when the sea is rough. Therefore, some devices on board buoys, such as PCs, satellite communication systems, and power systems, should be maintained without manning. Dual or triple settings of devices or alternative ways of operation in case of failure of one system would be a solution. Such autonomous systems should be developed for actual operation of the GNSS buoy system.

Second, the mechanical strength and stability of the buoy body should be maintained for a long time (*e.g.*, 10 years or more). This problem was discussed based on the 3-years and 7-months experiment

between 2013 and 2016 in Cape Muroto described in Section 6; for example, barnacles attached to the body of the buoy were examined to find out if they cause the changes in buoyancy or tilt. It was concluded, however, that there were no effects on the buoyancy or tilt of the buoy after the operation.[19] Additionally, in the above experiment, an examination was conducted to find out if ablation of the iron chain, which was used for mooring of the buoy to the anchor at the ocean floor, would lead to breakage out of friction caused by continuous swings of the chain because of the sea waves. However, the experiment showed that cautious design of the chain would prevent the chain from breaking even if the operation will be for 10 years or beyond. Lastly, an experiment was performed to find out if salty wind and water would cause earlier breakage of metallic material, but such problems may have to be solved using ocean civil engineering technologies. Considering these problems, it was concluded that it is possible to design a buoy sustainable over the long term even at the deep outer ocean at a depth of thousands of meters.[19]

Some care may have to be taken for loss of the buoy by, for example, crash with a vessel or vandalism. If the buoy drifts away from the original position, tracking the position of the buoy as it carries the GNSS is possible and can send messages of its coordinates.

A sufficient and stable power supply is a problem for the reliable long-term operation of the system. We designed the power system cautiously so that the system would work without sunshine for several days. However, the system stopped soon after our first deployment in November 2016. As discussed in Section 8, it was suspected that the shadow of the center pillar on the buoy, which is used for setting antennas of GNSS and satellite communication, would reduce the efficiency of electricity production of solar panels.[71] Tilting of the buoy due to waves might also reduce the efficiency of power generation. Careful design of the electric power supply with sufficient allowance is indispensable for long-term power supply on the buoy.

Another important factor for the reliable operation of GNSS buoys is the satellite communication link. In our previous experiments using Japanese Engineering Test Satellites (ETS-VIII), no serious problems were encountered, but the record indicated a correlation of frame-rate error, which means data loss, and wave height. This suggested that changes in the elevation angle between the antenna and the

satellite might affect the reliability of the data communication link. Careful examination of the cause of failure of the communication link is needed, as there are many causes for fading owing to the moving platform of the satellite antenna, as described in Section 6.[27]

When GNSS was developed for positioning in the 1970s, the required accuracy was at the level of meters by using the code of the GNSS signal. As a result of technical developments later, using the GNSS signal phase allowed positioning accuracy to be a few centimeters, and they can now be available in real time. Considering these new developments of GNSS technology together with satellite communication technology, we would be able to deploy GNSS buoys in any area of the ocean. Considering that the ocean has been considered as an area where data are difficult to be recorded, our GNSS buoy could serve as a significant change in fulfilling the gap in data distribution over the Earth's surface. Although our primary aim was to apply the technique for early tsunami detection, the recent development of our experiments added the GNSS buoy technique for observing ocean floor crustal movements. In addition to these applications, buoys placed in the ocean can be used for more applications. For example, the GNSS data can estimate precipitable water vapor (PWV) and total electron content (TEC) in the atmosphere and ionosphere, respectively, which are both important geophysical parameters.[19]

The PWV in the oceanic area is crucial for numerical weather forecasting through a four-dimensional data assimilation approach. Most of the data for the simulation have been taken on land. Considering that 70% of the Earth's surface is covered by the ocean, it is very important to include atmospheric parameters in the ocean area for data assimilation toward better weather forecasts. In Japan, PWV derived from GEONET of the GSI has already been used in numerical weather simulations. Inclusion of data from the surrounding oceanic region may improve the weather prediction by the simulation. GNSS PWV can be used with sufficient accuracy by placing GNSS on the ship. GNSS buoy could possess some merits compared with a ship as the buoy provides a fixed-point continuous data, relative to a moving irregularly observed shipborne data.[74],[75]

GNSS data recorded at a previous GNSS buoy station from Cape Muroto, southwest Japan, were used to show the tropospheric zenith delay; this was used to derive PWV, which can be used in atmospheric studies.[76] Shoji *et al.* (2018, unpub-
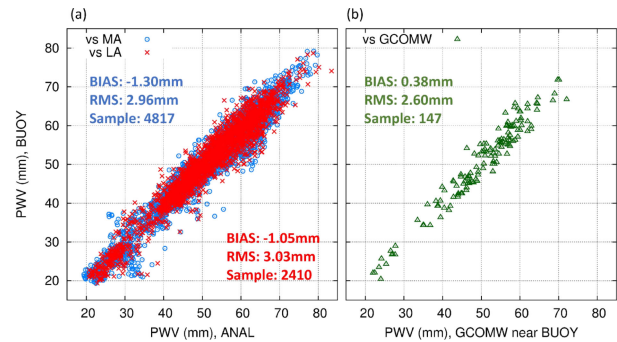

Fig. 22. (Color online) Precipitable water vapor (PWV) estimated at the buoy compared with (a) JMA objective analyses (MA: mesoscale analysis, LA: local analysis) and (b) Advanced Microwave Scanning Radiometer 2 (AMSR2) on board the Global Change Observation Mission 1st Water (GCOM-W1) (Shoji *et al.*, 2018, unpublished data).

lished data) examined how buoy-derived PWV is compatible with otherwise obtained PWV, using the data obtained between June 4 and September 15, 2018, in the present experiment. Figure 22 shows the comparison between the buoy PWV and (a) JMA's operational objective analyses (mesoscale analysis (MA) and local analysis) and (b) Advanced Microwave Scanning Radiometer 2 (AMSR2) on board the Global Change Observation Mission 1st Water (GCOM-W1) satellite data. These comparisons, in terms of their SDs showed that the differences between the buoy PWV and MA, LA, and GCOM-W1 were 2.96, 3.03, and 2.60 mm, respectively. The differences between the different methods were approximately 3 mm, suggesting that the inclusion of GNSS buoy data for data assimilation in weather forecasting could improve early warning systems of heavy rain such as linear rain bands and the prediction of typhoon paths.

The application of GNSS buoy data can also contribute to ionospheric research. For example, the National Institute of Information and Communications Technology of Japan (NICT) is conducting the Dense Regional and Worldwide International Networks of GNSS-TEC observation (DRAWING-TEC) project to develop high-resolution ionospheric TEC observations by collecting TEC data from dense GNSS array data.[77] They showed that such dense GNSS array data make it possible for ionospheric researchers to study medium-scale (100–1,000 km) ionospheric disturbances such as traveling ionospheric disturbances and equatorial plasma bubbles that are frequently observed in the mid- and low-latitude ionosphere. Moreover, high-resolution TEC maps
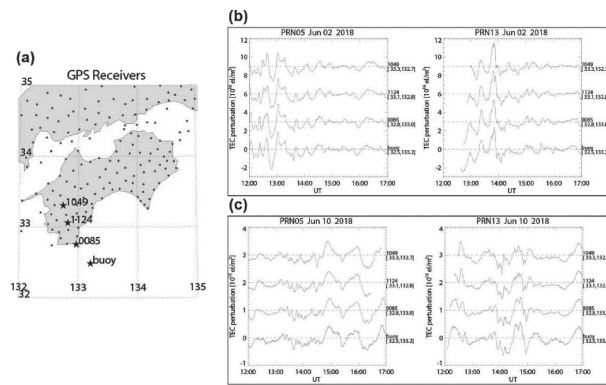
Fig. 23. Comparison of TEC variation. (a) Used sites of GEONET (1049, 1124, 0085) and GNSS buoy (buoy), estimated TEC variation for (b) PRN05 and PRN13 at UTC12-17 of June 2, 2018, and (c) PRN05 and PRN13 at UTC12-17 of June 10, 2018. Cases for (b) calm weather and (c) harsh weather (Tsugawa *et al.*, 2018; unpublished data).

Fig. 24. (Color online) Multipurpose GNSS buoy for synthetic geohazard monitoring, from ionosphere to ocean floor.[19]

can reveal ionospheric variations due to large earthquakes such as the 2011 Tohoku-oki earthquake.[78] Conversely, the ionospheric disturbances shown above may decrease position and navigation accuracy and hence lead to problems in land and air traffic. Thus, monitoring these ionospheric disturbances, known as a space weather phenomenon, is crucial for the integrity of GNSS system operation. GEONET is used to monitor ionospheric conditions in Japan during the operation of space weather forecasting services. However, the dense GNSS networks worldwide, which are used in their DRAWING-TEC project, are restricted to land, and more GNSS stations are needed in sparse areas, especially in the oceanic region.[77] Our efforts to develop GNSS buoys would help ionospheric research and space weather monitoring. Tsugawa *et al.* (2018, unpublished data) used a part of the data obtained in our buoy experiment in 2018 to derive ionospheric TEC values and showed that the ionospheric TEC variations have almost the same accuracy as that obtained by nearby GEONET sites (Fig. 23).

In studies on GNSS-TEC, both absolute and relative TEC values are used. The absolute TEC for the integrated electron density along the entire line of site (LOS) between the receiver and satellite was obtained using both the carrier phase and the GNSS code with corrections of satellite and receiver biases. The accuracy of the absolute TEC was expected to be several TECU (1 TECU = $\sim$54 ns = 16.2 cm).[79),80] The relative TEC is the perturbation component of absolute TEC by detrending it with a 1-h running average for each LOS. The accuracy of the relative
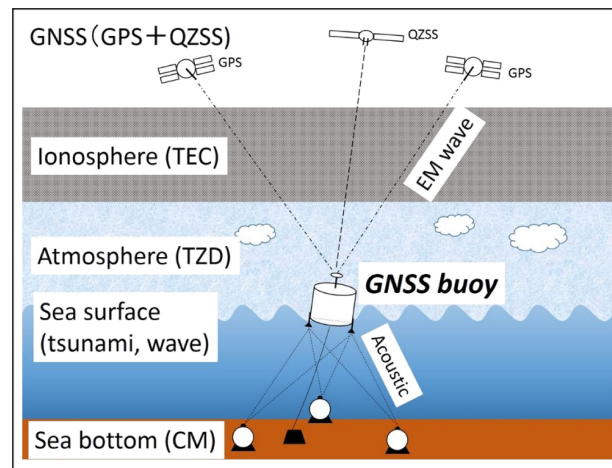
TEC ranged from 0.01 to 0.02 TECU, which corresponds to $\sim$1% of the wavelength of GPS signals L1 (0.19 m) and L2 (0.24 m).[81),82] Hence, relative TEC is widely used for monitoring ionospheric disturbances. Monitoring ionospheric disturbances for societal impact requires an accuracy of approximately 0.1 TECU (Tsugawa, 2021, personal communication). As shown in Fig. 23, the TEC perturbation of the buoy data clearly satisfies this requirement.

Summing up the possible applications of the GNSS buoy, a single buoy has a large potential for observing wide areas, covering from the ocean floor to the ionosphere. Geohazards related to space weather, atmospheric weather, sea surface waves, and crustal movements at the ocean floor can also be monitored using a single GNSS buoy. Thus, such a synthetic geohazard monitoring system using a GNSS buoy can be used as a monitoring tool (Fig. 24), and deployments of the array of GNSS buoys to a wide area in the northwestern Pacific area could serve as an important national infrastructure for geohazard monitoring systems and as a system of a new observation network for earth sciences (Fig. 25).[19] This hypothetical network is called as OCEAN GEONET, as compared with the GEONET, which has been widely used on land and has been operated by the GSI of Japan.[19]

If the construction of a GNSS buoy array in the ocean is adopted as a national project, many buoys should be placed around the Japanese coast, as shown in Fig. 24. The system may require a dedicated satellite that may have to be operated by
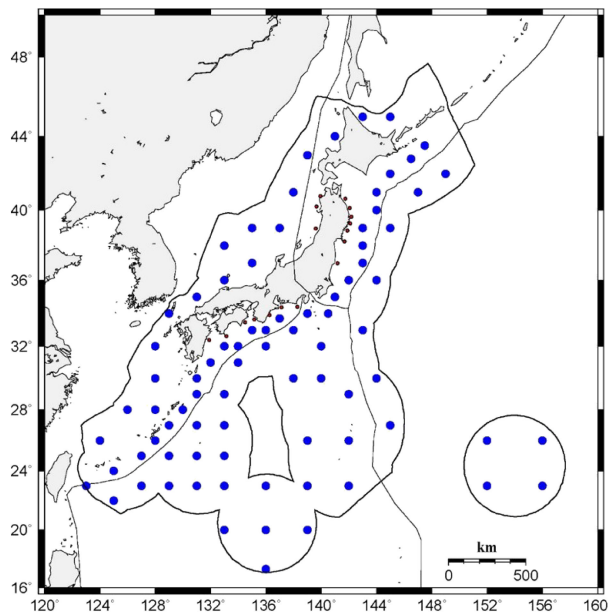
Fig. 25. (Color online) Future scope of GNSS buoy array in the northwestern Pacific. Small red dots are the currently operational GNSS buoy array for wave monitoring by NOWPHAS. Blue dots are arbitrarily plotted for a hypothetical GNSS buoy array. Solid lines indicate the Japanese Exclusive Economic Zone.[19]

the government, in which we might have to develop a new method for more effective satellite transmission technology. Recent technological development using the Internet of Things (IoT) Non-Terrestrial Network would be applicable for oceanic GNSS buoy arrays.[83]

Finally, we also discussed the cost of building and maintaining the entire system of the ocean array. The largest cost was attributed to the construction of the buoys. Constructing a buoy system will require several million U.S. dollars, although the price would be less if the number of orders are increased, for example, more than 80 buoys, as shown in Fig. 25. The cost of the satellite communication link is also a major component of the total cost. If a commercial satellite with 1 kbps is used, it may be possible to send buoy coordinates every second together with GNSS-A data for every 15 min, including other ancillary data such as temperature and gyro data. This may cost more than U.S.\$ 100,000 per year for a buoy. Ideally, the Japanese government should design a dedicated satellite system for sending and receiving data between the ground base and the buoys. In our experiment, we used a bidirectional data communication link. However, the cost of satellite communication could be much reduced if

the positioning satellite can send its precise orbit and clock. As the Japanese QZSS system is now in operational mode to send MADOCA, receiving and using MADOCA from QZSS on a buoy would significantly reduce the cost of data communication link. Operation of the ground station requires a high-performance computer and a large amount of storage with a backup system for sustainable operation. Therefore, given that 80 buoys will be constructed for OCEAN GEONET, construction of the total system would amount approximately to a few hundred million U.S. dollars for the buoys and an additional U.S.\$ 8 million per year for the data communication links. Including other ancillary devices and maintenance fees, the total cost for 10 years of operation is approximately several hundred million U.S. dollars.

11. Concluding remarks

Although OCEAN GEONET is still in the early stages of development, we hope it will materialize in the future. Although the construction of a buoy array in the ocean requires hundreds of millions of U.S. dollars, we would like to emphasize that it can provide a wide variety of earth scientists with unprecedented data of the ionosphere, atmosphere, sea-surface changes including tsunamis, and ocean-floor crustal deformations. Therefore, a GNSS buoy system will offer a highly cost-effective approach compared with other single-purpose-oriented projects to obtain new innovative data globally, thus beginning a new scientific innovation in the fields of solid earth, ocean, atmospheric, and ionospheric science.

Dr. Ken'ichi Takizawa, Dr. Morio Toyoshima, and Mr. Shin'ichi Yamamoto, of Network Research Institute, NICT,

Mr. Tadahiro Iwasaki and Mr. Naokiyo Koshikawa of JAXA.

The authors are indebted to members of the Fisheries Promotion Department in Kochi Prefecture for their assistance in using the Kuroboku buoys and to the staff members of Yuge-maru and Hamakaze of the National Institute of Technology, Yuge College, for their assistance during ship operations. The authors thank the staff of Hitachi Zosen Corporation, Softbank Corporation, and Kaiyo Gijutsu Co. Ltd. for their assistance during the course of this research. The authors are indebted to two anonymous reviewers and a handling editor who provided valuable comments to significantly improve the manuscript.

References

1) Kusano, F. and Yokota, T. (2011) History of tsunami warning services in Japan. Quart. J. Seismol. **74**, 35–91 (in Japanese).
2) Ozaki, T. (2011) Outline of the 2011 off the Pacific coast of Tohoku Earthquake (Mw 9.0) — Tsunami warnings/advisories and observations —. Earth Planets Space **63**, 827–830.
3) Bernard, E.N., Gonzalez, F.I., Meinig, C. and Miburn, H.G. (2001) Early detection and real-time reporting of deep-ocean tsunamis. In Proceedings of the International Tsunami Symposium 2001 (ITS 2001) (on CD-ROM), NTHMP Review Session, R-6, Seattle, WA, 7–10 August 2001, 97–108.
4) Hino, R., Tanioka, Y., Kanazawa, T., Sakai, S., Nishino, M. and Suyehiro, K. (2001) Micro-tsunami from a local interplate earthquake detected by cabled offshore tsunami observation in northeastern Japan. Geophys. Res. Lett. **28**, 3533–3536.
5) Hirata, K., Takahashi, H., Geist, E., Satake, K., Tanioka, Y., Sugioka, H. et al. (2003) Source depth dependence of micro-tsunamis recorded with ocean-bottom pressure gauges: the January 28, 2000 Mw 6.8 earthquake off Nemuro Peninsula, Japan. Earth Planet. Sci. Lett. **208**, 305–318.
6) Maeda, T., Furumura, T., Sakai, S. and Shinohara, M. (2011) Significant tsunami observed at ocean-bottom pressure gauges during the 2011 off the Pacific coast of Tohoku Earthquake. Earth Planets Space **63**, 803–808.
7) Kato, T., Terada, M., Kinoshita, M., Isshiki, H. and Yokoyama, A. (1998) A development of GPS tsunami meter. Gekkan Kaiyo **15** (Special Volume), 38–42 (in Japanese).
8) Kato, T., Terada, Y., Kinoshita, M., Kakimoto, H., Issiki, H., Matsuishi, M. et al. (2000) Real time observation of Tsunami by RTK-GPS. Earth Planets Space **52**, 841–845.
9) Born, G.H., Parke, M.E., Axelrad, P., Gold, K.L., Johnson, J., Key, K.W. et al. (1994) Calibration of the TOPEX altimeter using a GPS buoy. J. Geophys. Res. **99**, 24517–24526.
10) Shöne, T., Pandoe, W., Mudita, I., Roemer, S., Illigner, J., Zech, C. et al. (2011) GPS water level measurements for Indonesia's Tsunami Early Warning System. Nat. Hazards Earth Syst. Sci. **11**, 741–749.
11) Kato, T., Terada, Y., Ito, K., Hattori, R., Abe, T., Miyake, T. et al. (2005) Tsunami due to the 2004 September 5th off the Kii peninsula earthquake, Japan, recorded by a new GPS buoy. Earth Planets Space **57**, 297–301.
12) The Headquarters for Earthquake Research Promotion (1999) The Earthquake Activities of Japan, 391pp (in Japanese).
13) Terada, Y., Kato, T., Nagai, S., Koshimura, S., Miyake, T., Nishimura, H. et al. (2011) Development of a tsunami monitoring system using a GPS buoy. In Proceedings of International Global Navigation Satellite Systems Society IGNSS Symposium 2011, 411–422.
14) Kato, T., Terada, Y., Kinoshita, M., Kakimoto, H., Isshiki, H., Moriguchi, T. et al. (2001) A new tsunami monitoring system using RTK-GPS, In ITS 2001 Proceedings, Session 5, Number 5–12, pp. 645–651.
15) Kato, T., Terada, Y., Nishimura, H., Nagai, T. and Koshimura, S. (2011) Tsunami records due to the 2010 Chile Earthquake observed by GPS buoys established along the Pacific coast of Japan. Earth Planets Space **63**, e5–e8.
16) Watada, S. (2013) Tsunami speed variations in density-stratified compressible global oceans. Geophys. Res. Lett. **40**, 4001–4006.
17) Kawai, H., Satoh, M. and Kawaguchi, K. (2010) Annual report on Nationwide Ocean Wave Information Network for Ports and Harbours (NOWPHAS 2008). Tech. Note Port Airport Res. Inst. No. 1209, pp. 1–93 (in Japanese with English abstract).
18) Kawai, H., Satoh, M., Kawaguchi, K. and Seki, K. (2011) Characteristics of the 2011 off the Pacific Coast of Tohoku Earthquake tsunami. Rep. PARI **50**, 3–63 (in Japanese).
19) Kato, T., Terada, Y., Tadokoro, K., Kinugasa, N., Futamura, A., Toyoshima, M. et al. (2018) Development of GNSS buoy for a synthetic geohazard monitoring system. J. Disaster Res. **13**, 460–471.
20) Rocken, C., Mervart, L., Lukes, Z., Johnson, J., Kanzaki, H., Kakimoto, M. et al. (2004) Testing a new network RTK software system. In Proceedings of the 17th International Technical Meeting of the Satellite Division of the Institute of Navigation (ION GNSS 2004), U.S.A., pp. 2831–2839.
21) Mervart, L., Lukes, Z., Rocken, C. and Iwabuchi, T. (2008) Precise Point Positioning with Ambiguity Resolution in Real-Time. In Proceedings of the

21st International Technical Meeting of the Satellite Division of The Institute of Navigation (ION GNSS 2008), Savannah, GA, September 2008, pp. 397–405.

22) Zumberge, J., Heflin, M., Jefferson, D., Watkins, M. and Webb, F. (1997) Precise point positioning for the efficient and robust analysis of GPS data from large networks. J. Geophys. Res. **102**, 5005–5017.

23) Terada, Y., Kato, T., Nagai, T., Koshimura, S., Imada, N., Sakaue, H. *et al.* (2015) Recent developments of GPS tsunami meter for a far offshore observations. *In* Proceedings of the International Symposium on Geodesy for Earthquake and Natural Hazards (GENAH) (ed. Hashimoto, M.). International Association of Geodesy Symposia, Springer, Cham, Vol. 145, pp. 145–153.

24) Kato, T., Terada, Y., Tadokoro, K., Futamura, A., Toyoshima, M., Yamamoto, S. *et al.* (2017) GNSS buoy array in the ocean for a synthetic geohazards monitoring system. *In* Proceedings of the Twenty-seventh International Ocean and Polar Engineering Conference, San Francisco, CA, U.S.A., June 25–30, 2017, International Society of Offshore and Polar Engineers (ISOPE), ISOPE-I-17-213.

25) Yamamoto, S., Kawasaki, K., Terada, Y., Kato, T., Hashimoto, G., Motohashi, O. *et al.* (2014) Data transmission experiment from the buoy using the Engineering Test Satellite VIII (ETS-VIII) — The aim of early detection of Tsunami —. IEICE Tech. Rep. **114**, 5–10 (in Japanese).

26) Terada, Y., Yamamoto, S., Iwakiri, N., Iwasaki, K., Koshikawa, N., Tada, M. *et al.* (2016) An improvement of the antenna installation mechanism for satellite communication of the GPS tsunami meter. Presented at the JpGU 2016 Meeting, Chiba, May 2016, HDS19-24 (in Japanese).

27) Takizawa, K., Yamamoto, S., Toyoshima, M., Futamura, A., Terada, Y. and T. Katoh (2017) Channel modeling on satellite communications for GNSS buoy in the ocean. IEICE Tech. Rep. **117**, 99–102 (in Japanese).

28) Spiess, F.N. (1985) Suboeanic geodetic measurements. IEEE Trans. Geosci. Remote Sens. **GE-23**, 502–510.

29) Fujimoto, H. (2006) Ocean bottom crustal movement observation using GPS/Acoustic system by universities in Japan. J. Geod. Soc. Jpn. **52**, 265–272.

30) Fujita, M., Ishikawa, T., Mochizuki, M., Sato, M., Toyama, S., Katayama, M. *et al.* (2006) GPS/Acoustic seafloor geodetic observation: method of data analysis and its application. Earth Planets Space **58**, 265–275.

31) Tadokoro, K., Ando, M., Ikuta, R., Okuda, T., Besana, G.M., Sugimoto, S. *et al.* (2006) Observation of coseismic seafloor crustal deformation due to M7 class offshore earthquakes. Geophys. Res. Lett. **33**, L23306.

32) Ikuta, R., Tadokoro, K., Ando, M., Okuda, T., Sugimoto, S., Takatani, K. *et al.* (2008) A new GPS-Acoustic method for measuring ocean floor

crustal deformation: application to the Nankai Trough. J. Geophys. Res. **113**, B02401.

33) Spiess, F.N., Chadwell, C.D., Hildebrand, J.A., Young, L.E., Purcell, G.H., Jr. and Dragert, H. (1998) Precise GPSrAcoustic positioning of seafloor reference points for tectonic studies. Phys. Earth Planet. Inter. **108**, 101–112.

34) Chadwell, C.D. and Spiess, F.N. (2008) Plate motion at the ridge-transform 326 boundary of the south Cleft segment of the Juan de Fuca Ridge from GPS-Acoustic data. J. Geophys. Res. **113**, B04415.

35) Yasuda, K., Tadokoro, K., Taniguchi, S., Kimura, H. and Matsuhiro, K. (2017) Interplate locking condition derived from seafloor geodetic observation in the shallowest subduction segment at the Central Nankai Trough, Japan. Geophys. Res. Lett. **44**, 3572–3579.

36) Chen, H.-Y., Ikuta, R., Lin, C.-H., Hsu, Y.-J., Kohmi, T., Wang, C.-C. *et al.* (2018) Back-arc opening in the western end of the Okinawa Trough revealed from GNSS/Acoustic Measurements. Geophys. Res. Lett. **45**, 137–145.

37) Gagnon, K., Chadwell, C.D. and Norabuena, E. (2005) Measuring the onset of locking in the Peru-Chile trench with GPS and acoustic measurements. Nature **434**, 205–208.

38) Fujita, M., Ishikawa, T., Mochizuki, M., Sato, M., Toyama, S., Katayama, M. *et al.* (2006) GPS/Acoustic seafloor geodetic observation: method of data analysis and its application. Earth Planets Space **58**, 265–275.

39) Matsumoto, Y., Ishikawa, T., Fujita, M., Sato, M., Saito, H., Mochizuki, M. *et al.* (2008) Weak interplate coupling beneath the subduction zone off Fukushima, NE Japan, inferred from GPS/acoustic seafloor geodetic observation. Earth Planets Space **60**, e9–e12.

40) Tadokoro, K., Ikuta, R., Watanabe, T., Ando, M., Okuda, T., Nagai, S. *et al.* (2012) Interseismic seafloor crustal deformation immediately above the source region of anticipated megathrust earthquake along the Nankai Trough. Japan. Geophys. Res. Lett. **39**, L10306.

41) Tadokoro, K., Nakamura, M., Ando, M., Kimura, H., Watanabe, T. and Matsuhiro, K. (2018) Interplate coupling state at the Nansei-Shoto (Ryukyu) Trench, Japan, deduced from seafloor crustal deformation measurements. Geophys. Res. Lett. **45**, 6869–6877.

42) Watanabe, S., Sato, M., Fujita, M., Ishikawa, T., Yokota, Y., Ujihara, N. *et al.* (2014) Evidence of viscoelastic deformation following the 2011 Tohoku-Oki earthquake revealed from seafloor geodetic observation. Geophys. Res. Lett. **41**, 5789–5796.

43) Watanabe, S., Bock, Y., Melgar, D. and Tadokoro, K. (2018) Tsunami scenarios based on interseismic models along the Nankai trough, Japan, from seafloor and onshore geodesy. J. Geophys. Res. **123**, 2448–2461.

44) Yasuda, K., Tadokoro, K., Ikuta, R., Watanabe, T., Nagai, S., Okuda, T. *et al.* (2014) Interplate

locking condition derived from seafloor geodetic data at the northernmost part of the Suruga Trough, Japan. Geophys. Res. Lett. **41**, 5806–5812.

45) Yokota, Y., Ishikawa, T., Sato, M., Watanabe, S., Saito, H., Ujihara, N. *et al.* (2015) Heterogeneous interplate coupling along the Nankai Trough, Japan, detected by GPS-acoustic seafloor geodetic observation. Prog. Earth Planet. Sci. **2**, 10.

46) Yokota, Y., Ishikawa, T., Watanabe, S., Tashiro, T. and Asada, A. (2016) Seafloor geodetic constraints on interplate coupling of the Nankai Trough megathrust zone. Nature **534**, 374–377.

47) Nishimura, T., Yokota, Y., Tadokoro, K. and Ochi, T. (2018) Strain partitioning and interplate coupling along the northern margin of the Philippine Sea plate, estimated from Global Navigation Satellite System and Global Positioning System-Acoustic data. Geosphere **14**, 535–551.

48) Kimura, H., Tadokoro, K. and Ito, T. (2019) Interplate coupling distribution along the Nankai Trough in southwest Japan estimated from the block motion model based on onshore GNSS and seafloor GNSS/A observations. J. Geophys. Res. **124**, 6140–6164.

49) Kido, M., Fujimoto, H., Miura, S., Osada, Y., Tsuka, K. and Tabei, T. (2006) Seafloor displacement at Kumano-nada caused by the 2004 off Kii Peninsula earthquakes, detected through repeated GPS/Acoustic surveys. Earth Planets Space **58**, 911–915.

50) Kido, M., Osada, Y., Fujimoto, H., Hino, R. and Ito, Y. (2011) Trenchnormal variation in observed seafloor displacements associated with the 2011 Tohoku-Oki earthquake. Geophys. Res. Lett. **38**, L24303.

51) Tadokoro, K., Ando, M., Ikuta, R., Okuda, T., Besana, G.M., Sugimoto, S. *et al.* (2006) Observation of coseismic seafloor crustal deformation due to *M*7 class offshore earthquakes. Geophys. Res. Lett. **33**, L23306.

52) Matsumoto, Y., Fujita, M., Ishikawa, T., Mochizuki, M., Yabuki, T. and Asada, A. (2006) Undersea co-seismic crustal movements associated with the 2005 Off Miyagi Prefecture Earthquake detected by GPS/acoustic seafloor geodetic observation. Earth Planets Space **58**, 1573–1576.

53) Sato, M., Saito, H., Ishikawa, T., Matsumoto, Y., Fujita, M., Mochizuki, M. *et al.* (2011) Restoration of interplate locking after the 2005 Off-Miyagi Prefecture earthquake, detected by GPS/acoustic seafloor geodetic observation. Geophys. Res. Lett. **38**, L01312.

54) Tomita, F., Kido, M., Osada, Y., Hino, R., Ohta, Y. and Iinuma, T. (2015) First measurement of the displacement rate of the Pacific Plate near the Japan Trench after the 2011 Tohoku-Oki earthquake using GPS/acoustic technique. Geophys. Res. Lett. **42**, 8391–8397.

55) Tomita, F., Kido, M., Ohta, Y., Iinuma, T. and Hino, R. (2017) Along-trench variation in seafloor displacements after the 2011 Tohoku earthquake. Sci. Adv. **3**, e1700113.

56) Iinuma, T., Hino, R., Uchida, N., Nakamura, W., Kido, M., Osada, Y. *et al.* (2016) Seafloor observations indicate spatial separation of coseismic and postseismic slips in the 2011 Tohoku earthquake. Nat. Commun. **7**, 13506.

57) Sato, M., Ishikawa, T., Ujihara, N., Yoshida, S., Fujita, M., Mochizuki, M. *et al.* (2011) Displacement above the hypocenter of the 2011 Tohoku-oki earthquake. Science **332**, 1395.

58) Iinuma, T., Hino, R., Kido, M., Inazu, D., Osada, Y., Ito, Y. *et al.* (2012) Coseismic slip distribution of the 2011 off the Pacific Coast of Tohoku Earthquake (M9.0) refined by means of seafloor geodetic data. J. Geophys. Res. **117**, B07409.

59) Kido, M., Fujimoto, H., Hino, R., Ohta, Y., Osada, Y., Iinuma, T. *et al.* (2015) Progress in the project for development of GPS/Acoustic technique over the Last 4 years. *In* Proceeding of the International Symposium on Geodesy for Earthquake and Natural Hazards (GENAH) (ed. Hashimoto, M.). International Association of Geodesy Symposia, Springer, Cham, Vol. 145, pp. 3–10.

60) Kido, M., Imano, M., Ohta, Y., Fukuda, T., Takahashi, N., Tsubone, S. *et al.* (2018) Onboard realtime processing of GPS-acoustic data for moored buoy-based observation. J. Disaster Res. **13**, 472–488.

61) Imano, M., Kido, M., Honsho, C., Ohta, Y., Takahashi, N., Fukuda, T. *et al.* (2019) Assessment of directional accuracy of GNSS-Acoustic measurement using a slackly moored buoy. Prog. Earth Planet. Sci. **6**, 56.

62) Chadwell, C.D. (2013) GPS-Acoustic Seafloor Geodesy using a Wave Glider. Abstract G14A-01 presented at 2013 Fall Meeting, AGU, San Francisco, Calif., 9–13 Dec. 2013.

63) Sathiakumar, S., Barbot, S., Hill, E., Peng, D., Zerucha, J., Suhaimee, S. *et al.* (2016) Seafloor geodesy using wave gliders to study earthquake and tsunami hazards at subduction zones. Abstract G31A-1046 presented at 2016 Fall Meeting, AGU, San Francisco, Calif., 11–15 Dec. 2016.

64) Iinuma, T., Kido, M., Ohta, Y., Fukuda, T., Tomita, F. and Ueki, I. (2021) GNSS-Acoustic observations of seafloor crustal deformation using a wave glider. Front. Earth Sci. **9**, 600946.

65) Cruz-Atienza, V.M., Ito, Y., Kostoglodov, V., Hjörleifsdóttir, Iglesias, A., Tago, J. *et al.* (2018) A seismogeodetic amphibious network in the Guerrero seismic gap, Mexico. Seismol. Res. Lett. **89**, 1435–1449.

66) Kinugasa, N., Tadokoro, K., Inagaki, S., Terada, Y., Futamura, A. and Kato, T. (2018) Development of acoustic signal processing unit for continuous observation of ocean bottom crustal deformation using marine GNSS buoy. Presented at the JpGU 2018 Meeting, SCG67-P06.

67) Kido, M. (2007) Detecting horizontal gradient of sound speed in ocean. Earth Planets Space **59**, e33–e36.

68) Kinugasa, N., Tadokoro, K., Kato, T. and Terada, Y.

(2020) Estimation of temporal and spatial variation of sound speed in ocean from GNSS-A measurements for observation using moored buoy. Prog. Earth Planet. Sci. **7**, 21.

69) Isshiki, H., Tsuchiya, A., Kato, T., Terada, Y., Kakimoto, H., Kinoshita, M. *et al.* (2000) Precise variance detection by a single GPS receiver — PVD (Point precise Variance Detection) Method —. J. Geod. Soc. Jpn. **46**, 239–251.

70) Becker, J.J., Sandwell, D.T., Smith, W.H.F., Braud, J., Binder, B., Depner, J. *et al.* (2009) Global bathymetry and elevation data at 30 arc seconds resolution: SRTM30_PLUS. Mar. Geod. **32**, 355–371.

71) Tadokoro, K., Kinugasa, N., Kato, T., Terada, Y. and Matsuhiro, K. (2020) A marine-buoy-mounted system for continuous and real-time measurement of seafloor crustal deformation. Front. Earth Sci. **8**, 123.

72) Tadokoro, K., Kinugasa, N., Kato, T., Terada, Y. and Matsuhiro, K. (2021) Buoy-mounted system for continuous and real-time seafloor crustal deformation measurements. Presented at the JpGU-AGU2020 meeting, July 2021.

73) Watanabe, S., Ishikawa, T., Yokota, Y. and Nakamura, Y. (2020) GARPOS: Analysis Software for the GNSS — A seafloor positioning with simultaneous estimation of sound speed structure. Front. Earth Sci. **8**, 597532.

74) Shoji, Y., Sato, K., Yabuki, M. and Tsuda, T. (2016) PWV Retrieval over the ocean using shipborne GNSS receivers with MADOCA real-time orbits. Sci. Online Lett. Atmos. **12**, 265–271.

75) Shoji, Y., Sato, K., Yabuki, M. and Tsuda, T. (2017) Comparison of shipborne GNSS-derived precipitable water vapor with radiosonde in the western North Pacific and in the sea adjacent to Japan. Earth Planets Space **69**, 153.

76) Shoji, Y. (2010) The experiment of the tropospheric zenith delay analysis using the GPS tsunami buoy off Cape Muroto, Japan. Presented at the 2010 Spring Meeting of the Meteorological Society of Japan, 23rd May 2010, Tokyo, Japan.

77) Tsugawa, T., Nishioka, M., Ishii, M., Hozumi, K., Saito, S., Shinbori, A. *et al.* (2018) Total Electron Content observations by dense regional and worldwide international networks of GNSS. J. Disaster Res. **13**, 535–545.

78) Tsugawa, T., Saito, A., Otsuka, Y., Nishioka, M., Maruyama, T., Kato, H. *et al.* (2011) Ionospheric disturbances detected by GPS total electron content observation after the 2011 off the Pacific coast of Tohoku Earthquake. Earth Planets Space **63**, 875–879.

79) Otsuka, Y., Ogawa, T., Saito, A., Tsugawa, T., Fukao, S. and Miyazaki, S. (2002) A new technique for mapping of total electron content using GPS network in Japan. Earth Planets Space **54**, 63–70.

80) Sekido, M., Kondo, T. and Kawai, E. (2003) Evaluation of GPS-based ionospheric TEC map by comparing with VLBI data. Raido Sci. **38**, 1069.

81) Tsugawa, T., Otsuka, Y., Coster, A.J. and Saito, A. (2007) Medium-scale traveling ionospheric disturbances detected with dense and wide TEC maps over North America. Geophys. Res. Lett. **34**, L22101.

82) Spilker, J., Jr. and Parkinson, B.W. (1996) Overview of GPS operation and design. *In* Global Positioning System: Theory and Applications (eds. Parkinson, B.W. and Spilker, J., Jr.). American Institute of Aeronautics and Astronautics, Inc., Reston, Va, Vol. 1, pp. 29–55.

83) Takizawa, K., Yamamoto, S., Terada, Y. and Kato, T. (2021) Non-Orthogonal Multiple Access (NOMA) in IoT Non-Terrestrial-Network for GNSS buoy array in the ocean. Presented at the IEEE VTC2021-Fall meeting, 27–30 September 2021.

Profile

Teruyuki Kato was born in Kanagawa Prefecture in 1952. He received his M.S. and Ph.D. in 1977 and 1980, respectively, from the University of Tokyo. He started his research career as a Japan Society for the Promotion of Science (JSPS) Postdoctoral Research Fellow at the Earthquake Research Institute (ERI), the University of Tokyo, and was soon hired as an assistant professor at ERI in 1980. He was promoted to associate professor in 1991 and then to a professor in 2000 at the same institute. His research field is geodesy, and he is studying the application of the Global Navigation Satellite System (GNSS) for crustal deformation research and for developing a GNSS buoy for early tsunami warning. After retirement from the University of Tokyo in 2018, he worked as the Director at the Hot Springs Research Institute of Kanagawa Prefecture from 2018 to 2021.

He is a specially appointed professor at Taisho University, Tokyo, Japan.

Profile

Yukihiro Terada was born in Ehime Prefecture in 1949 and graduated from Osaka University in 1972. He started his research career as an engineer at the Technical Research Institute, Hitachi Zosen Corporation. He was engaged in developing non-destructive examination method and apparatus for the material and welded joints of steel structures. For these achievements, he was granted a Ph.D. by the Kyushu Institute of Technology in 1995. He started to develop a tsunami meter using GNSS technology after the 1995 Southern Hyogo Prefecture Earthquake. He was commended by the Minister of Land, Infrastructure, Transport and Tourism for the development of a GNSS tsunami monitoring system in 2004.

Yukihiro Terada was invited to the National Institute of Technology, Kochi College, as a professor in 2006. He has been an honorary professor and visiting professor there since 2015.

Profile

Keiichi Tadokoro was born in Hyogo Prefecture in 1973. He received his M.S. and Ph.D. degrees from Kyoto University in 1997 and 2000, respectively. In his doctoral thesis, he investigated temporal variations in the structure and physical properties of a fault zone from seismic wave analyses. He became a research associate (assistant professor) at the Earthquake and Volcano Research Center, Graduate School of Environmental Studies, Nagoya University, in 2000. He was promoted to associate professor in 2006. He has contributed to the development of a measurement system for sea-floor crustal deformation using the GNSS-Acoustic technique. His current research topic is the interplate coupling along the Nankai Trough and the Ryukyu Trench derived from sea-floor crustal deformation. He is also developing an advanced system for GNSS-Acoustic measurements.

Profile

Akira Futamura was born in Aichi Prefecture in 1974. He received his M.S. from the Tokyo University of Mercantile Marine in 2000. His Ph.D. was obtained from Ehime University in 2005. He started his research career as a research associate at the National Institute of Technology, Yuge College, in 2000. He was promoted to associate professor in 2008 and a professor in 2020 at the National Institute of Technology, Yuge College. He has conducted research on the marine environment in the Seto Inland Sea in the field of coastal oceanography. In addition, he is conducting research in the field of seafarer education.